Visualizing Long-Term Memory Formation in Two Neurons of the *Drosophila* Brain

Chun-Chao Chen, *et al.*

Science **335**, 678 (2012);
DOI: 10.1126/science.1212735

Visualizing Long-Term Memory Formation in Two Neurons of the *Drosophila* Brain

Chun-Chao Chen,[1] Jie-Kai Wu,[1] Hsuan-Wen Lin,[1] Tsung-Pin Pai,[1] Tsai-Feng Fu,[3] Chia-Lin Wu,[2] Tim Tully,[4] Ann-Shyn Chiang[1,2,5,6]*

Long-term memory (LTM) depends on the synthesis of new proteins. Using a temperature-sensitive ribosome-inactivating toxin to acutely inhibit protein synthesis, we screened individual neurons making new proteins after olfactory associative conditioning in *Drosophila*. Surprisingly, LTM was impaired after inhibiting protein synthesis in two dorsal-anterior-lateral (DAL) neurons but not in the mushroom body (MB), which is considered the adult learning and memory center. Using a photoconvertible fluorescent protein KAEDE to report de novo protein synthesis, we have directly visualized cyclic adenosine monophosphate (cAMP) response element–binding protein (CREB)–dependent transcriptional activation of *calcium/calmodulin-dependent protein kinase II* and *period* genes in the DAL neurons after spaced but not massed training. Memory retention was impaired by blocking neural output in DAL during retrieval but not during acquisition or consolidation. These findings suggest an extra-MB memory circuit in *Drosophila*: LTM consolidation (MB to DAL), storage (DAL), and retrieval (DAL to MB).

In *Drosophila*, LTM is produced by spaced repetitive training, which induces cyclic adenosine monophosphate (cAMP) response element–binding protein (CREB)–dependent gene transcription followed by de novo protein synthesis (*1*, *2*). A prominent neuroanatomical site involved with memory formation is the mushroom body (MB), which consists of γ, α′β′, and αβ neurons. Calcium-imaging studies have shown that each cell type displays a distinct and altered activity at different time durations after training (*3*). Moreover, 30 different genetic or pharmacological disruptions have suggested that the MBs are involved in both short-term memory (STM) and long-term memory (LTM) (*3*–*8*). Nevertheless, de novo protein synthesis required for LTM consolidation has never been directly visualized and/or manipulated in any targeted brain structures, including the MBs.

Visualizing de novo protein synthesis in targeted neurons. KAEDE is a green fluorescent protein (GFP), which changes its structure irreversibly to a red fluorescent protein (RFP) upon ultraviolet (UV) irradiation (*9*, *10*). We generated a transgenic *upstream activation sequence* (*UAS*)–*kaede* to monitor de novo transcriptional activities in targeted neurons. We showed that KAEDE faithfully reports the cyclic transcriptional activity of *period* (*per*) in circadian pacemaker cells (lateral neurons). Preexisting green KAEDE in the lateral neurons was photoconverted into red KAEDE in living *per-Gal4>UAS-kaede* flies exposed to UV irradiation (fig. S1, A and B). By photoconverting green KAEDE to red every 4 hours, we showed that KAEDE exhibits a diurnal cycle of de novo synthesis in the lateral neurons (Fig. 1A), parallel to the oscillation of *per* RNA (*11*). Newly synthesized green KAEDE was about 10 times as high during the night as during the day, indicated by accumulative measurement (Fig. 1A) and time lapse recording (movie S1). This de novo KAEDE synthesis in lateral neurons was reduced significantly in flies fed the protein synthesis inhibitor, cycloheximide (Fig. 1B). In contrast, red KAEDE remained at a constant level with or without cycloheximide feeding, confirming that photoconverted red KAEDE is irreversible and that spontaneous conversion of green KAEDE to red does not occur.

RICIN is a potent cytotoxic protein that inactivates eukaryotic ribosomes by hydrolytically cleaving the N-glycosidic bond (A^{4324}) of the 28*S* ribosomal RNA subunit (*12*, *13*). We obtained an effective transgenic fly carrying a cold-sensitive *UAS-ricin*^{CS} transgene, by remobilization of a P-element insertion generated previously (*14*). In *OK107-Gal4>UAS-ricin*^{CS} flies, high-temperature (30°C) RICIN^{CS} inactivated ribosomes, causing a severe MB deformation; at low temperature (18°C), however, RICIN^{CS} itself was inactive, thereby allowing normal MB development (fig. S1C).

We also visualized the effect of RICIN^{CS} on protein synthesis using KAEDE as a reporter. Using *per-Gal4* as a driver, we found that KAEDE synthesis in lateral neurons was not inhibited by RICIN^{CS} at 18°C but decreased ~80% by RICIN^{CS} at 30°C for at least 5 hours (Fig. 1C). KAEDE synthesis inhibited by activated RICIN^{CS} at permissive temperature is quickly restored to normal level after a shift to the toxin's restrictive temperature, suggesting that working ribosomes are resynthesized (Fig. 1C). Similar effects of RICIN^{CS} inhibition of protein synthesis were found in MB neurons (Fig. 1, D and E), using *OK107-Gal4*, which likely labels all MB neurons, and choline acetyltransferase (*Cha*) promoter–driving *Gal4*, which likely labels most acetylcholine-producing neurons.

Behavioral screen for neurons involved in protein synthesis–dependent memory formation. The spatiotemporal precision of *UAS-ricin*^{CS} for acutely blocking protein synthesis in small subsets of targeted neurons allowed us to identify neurons undergoing protein synthesis during LTM formation. RICIN^{CS} activated (30°C) immediately after spaced training in *Cha-Gal4* that contains ~60% of total brain neurons (*15*) impaired 1-day memory (Fig. 2A). The impairment was specific to LTM rather than anesthesia-resistant memory (ARM), because cycloheximide fed to these flies did not further reduce 1-day memory after spaced training and because activated RICIN^{CS} did not impair 1-day memory after massed training.

In this form of associative learning, olfactory information (the conditioned stimulus) is detected by sensory neurons and then is relayed by projection neurons from the antennal lobe to the MB, where it is modulated by anterior paired lateral (APL) and dorsal paired medial (DPM) neurons. Through uncharacterized interneurons, information processed in the MBs eventually reaches the central complex, including the ellipsoid body. Foot-shock punishment (the unconditioned stimulus) is thought to reach MB through dopaminergic *TH-Gal4* neurons (*16*–*18*). Unexpectedly, 1-day memory retention remained intact when RICIN^{CS} was expressed in olfactory sensory neurons (*Or83b-Gal4*), olfactory projection neurons (*GH146-Gal4*), MB modulatory neurons (*GH146-Gal4, c316-Gal4*), all MB neurons (*c247-Gal4*, *c772-Gal4*, and *OK107-Gal4*), αβ neurons (*c739-Gal4*), α′β′ neurons (*c305a-Gal4*, *E0973-Gal4*, and *G0050-Gal4*), ellipsoid body neurons (*c42-Gal4*, *c217-Gal4*, *c507-Gal4*, *Feb170-Gal4*, and *P0010-Gal4*) and dopaminergic neurons (*TH-Gal4*) and again activated immediately after spaced training (Fig. 2B). Furthermore, by limiting RICIN^{CS} expression to neurons outside of MB using a combination of *Cha-Gal4* and *MB-Gal80* (Gal80 inhibits Gal4), 1-day memory again was impaired when RICIN^{CS} was activated immediately after spaced training but not after massed training (Fig. 2C and fig. S2A). Therefore, regardless of numerous studies suggesting LTM storage in the antennal lobes (*19*), the MBs (*3*, *20*) and the ellipsoid body (*21*), our results suggest that de novo protein synthesis during LTM formation occurs in *Cha-Gal4*–expressing neurons outside of the MBs.

Next, we performed a more extensive behavioral screen for patterns of RICIN^{CS} expression that yielded 1-day memory impairments when RICIN^{CS} was activated immediately after spaced training (fig. S2B). LTM was impaired with *Gal4*

[1]Institute of Biotechnology and Department of Life Science, National Tsing Hua University, Hsinchu 30013, Taiwan. [2]Brain Research Center, National Tsing Hua University, Hsinchu 30013, Taiwan. [3]Department of Applied Chemistry, National Chi Nan University, Nantou 54561, Taiwan. [4]Dart Neuroscience, LLC, 7374 Lusk Boulevard, San Diego, CA 92121, USA. [5]Genomics Research Center, Academia Sinica, Nankang, Taipei 11529, Taiwan. [6]Kavli Institute for Brain and Mind, University of California at San Diego, La Jolla, CA 92093–0526, USA.

*To whom correspondence should be addressed. E-mail: aschiang@life.nthu.edu.tw

drivers, *cer* (*crammer*)-, *Ddc* (*Dopa decarboxylase*)-, *Trh493* (*Tryptophan hydroxylase*)-, *Trh996*-, *cry* (*cryptochrome*)-, *per*-, *CaMKII*-(X), and *CaMKII-Gal4*(III), whereas LTM was normal with *Gal4* drivers, *DVGLUT* (*Vesicular glutamate transporter*)-, *Gad* (*Glutamic acid decarboxylase 1*)-, *tim* (*timeless*)*14-27*-, *tim14-82*-, and *repo* (*reversed polarity*)–*Gal4*, the latter of which labels glial cells (Fig. 2B). LTM impairments by activated RICIN^{CS} in targeted *Gal4* neurons were confirmed again by repeating the experiment using "Cantonized" *Gal4* lines outcrossed to control flies to equilibrate genetic backgrounds (fig. S3).

Identification of individual neurons with protein synthesis during LTM formation. PER protein is necessary for LTM after courtship conditioning (*22*, *23*). We found that PER protein was also necessary for LTM after olfactory conditioning. In *per*^{0} flies, 1-day memory retention was impaired after spaced, but not after massed, training (fig. S4A). In contrast, 1-day memory after spaced training was normal in other circadian mutants, including *tim*^{03}, *tim*^{04}, *dClk*^{Jrk}, and *cyc*^{0} (fig. S4B). By blocking neurotransmission with *UAS-shi*^{ts}, a temperature-sensitive dynamin protein (*24*, *25*), we found that neural activity from *per* neurons was required for retrieval of 1-day memory after spaced training but not 3 hours or immediately after a single training session (fig. S4C). Activation of RICIN^{CS} in *per* neurons impaired 1-day memory after spaced training but not after massed training (fig. S4D). Moreover, by activating RICIN^{CS} in *per* neurons at different time windows after spaced training, we found that protein synthesis was required only during the first 12 hours of LTM formation (fig. S4D). We also evaluated activated RICIN^{CS} in MB neurons (*OK107-Gal4* and *c247-Gal4*) using a sliding 12-hour window before and after spaced training (fig. S5). One-day memory retention remained normal in every case.

We identified individual neurons by looking for overlap in expression patterns of the 9 *Gal4* driver lines in which activated RICIN^{CS} impaired LTM formation. *Ddc-Gal4* and *per-Gal4* were chosen for the initial analysis because of their distinctly different expression patterns (fig. S2B). Two *per-Gal4* neurons located at the dorsal-anterior-lateral (DAL) protocerebrum and most *Ddc-Gal4* neurons were immunopositive for DDC antibodies (fig. S6A). The two DAL neurons are good candidates for their participation in protein synthesis–dependent LTM formation because they also express *N*-methyl-D-aspartate (NMDA) receptors (dNR), which are required for LTM formation (*26*). DDC-antibody immunostaining, in fact, revealed that the DAL neurons are included in the expression patterns of all nine *Gal4* driver lines (Fig. 3A). We also used *cry-Gal80* to "subtract" expression of RICIN^{CS} in the two DAL neurons from *Cha-Gal4* and *per-Gal4* expression patterns (Fig. 3, B and C, and fig. S6B). In both cases, activated RICIN^{CS} in the remaining neurons did not affect 1-day memory after spaced training (Fig. 3, D and E), suggesting that protein synthesis for LTM formation occurred in neurons within the intersection of the *Cha-Gal4*, *per-Gal4* and *cry-Gal80* expression patterns, including the two DAL neurons. Next, we identified three new *Gal4* drivers (*E0946, G0338,* and *G0431*) with relatively limited patterns of expression, but each of which contained the DAL neurons (validated again by DDC-antibody immunostaining) (Fig. 3F). In all three cases, we found that RICIN^{CS}, when activated during the first 12 hours after training, disrupted 1-day memory after spaced training but not after massed training (Fig. 3G).

Using the same three *Gal4* drivers (*E0946, G0338,* and *G0431*), we then used *UAS-shi*^{ts} acutely to block neurotransmission from DAL neurons. One-day memory after spaced training was normal when neurotransmission was blocked (i) from 30 min before training to the first 8 hours after training, (ii) 8 to 16 hours after training, or (iii) 16 to 24 hours after training (Fig. 3H). Instead, retrieval of LTM was disrupted when neurotransmission was blocked during the test trial 1 day after spaced training (Fig. 3H). Blocking neurotransmission from DAL with these three *Gal4* drivers did not affect memory retrieval immediately or 3 hours after one training session (fig. S7).

Are there other neurons that undergo protein synthesis during LTM formation? We used *cry-Gal80* to subtract expression of RICIN^{CS} in DAL neurons from the broader expression patterns of a panel of *Gal4* driver lines. When *cry-Gal80* was combined with *cer-Gal4* and RICIN^{CS} was activated for 24 hours immediately after training, 1-day memory after spaced training was defective and 1-day memory after massed training was

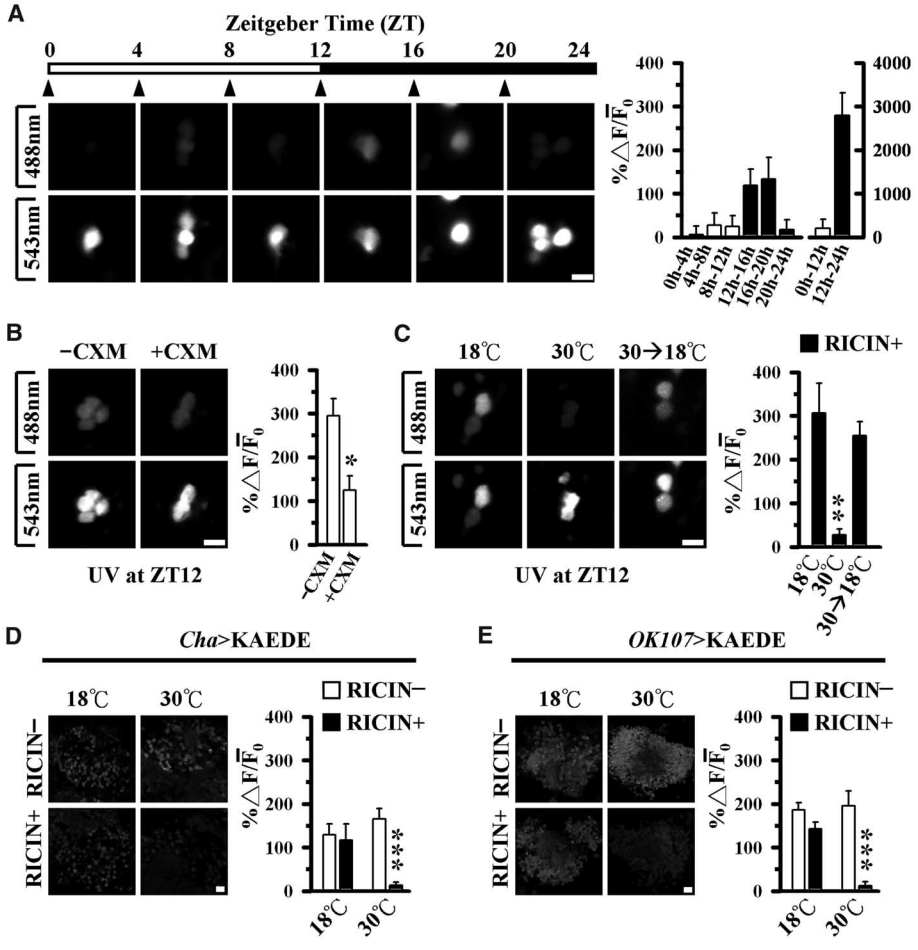

Fig. 1. Visualizing and blocking de novo protein synthesis in identified neurons. (**A**) Diurnal cycle of *per* transcriptional activity in the lateral neurons. To reset preexisting green KAEDE, living flies were UV irradiated every 4 hours (arrowheads) or every 12 hours, i.e., Zeitgeber Time (ZT) 0 or 12. Measurement of relative amount of de novo KAEDE synthesis was estimated within flies by normalizing to preexisting red KAEDE (%$\Delta F/\bar{F}_0$). Values are means ± SEM (N = 3 to 7 samples). (**B**) The effect of cycloheximide (+CXM) feeding. Images of lateral neurons were taken 5 hours after photoconversion at ZT12. Values are means ± SEM (N = 8 to 24 samples; *, $P < 0.05$). (**C**) The effect of activated RICIN^{CS}. Flies were photoconverted at ZT12 and kept (i) at 18°C (inactive RICIN^{CS}), (ii) at 30°C (activated RICIN^{CS}) during ZT12 to ZT17, or (iii) at 30°C during ZT7 to ZT12 and at 18°C during ZT12 to ZT17. Images of lateral neurons were taken at ZT17. Values are means ± SEM (N = 6 to 16 samples; *, $P < 0.05$; **, $P < 0.01$). (**D** and **E**) Effects of activated RICIN^{CS} in the MB neurons. After photoconversion, flies were kept at 18°C or 30°C for 24 hours before imaging. Values are means ± SEM (N = 10 to 15 samples; ***, $P < 0.001$). For all images, scale bar represents 10 μm. See supporting online material for more detailed legends of this and the other figures.

normal (fig. S8A), indicating that other neurons within the *cer* expression pattern also undergo de novo protein synthesis along with DAL neurons during LTM formation. In contrast, when *cry-Gal80* was combined with *Cha-Gal4*, *Ddc-Gal4*, *Trh493-Gal4*, *Trh996-Gal4*, *cry-Gal4*, *per-Gal4*, *CaMKII-Gal4*(X) or *CaMKII-Gal4*(III) and RICIN^{CS} was activated for 24 hours immediately after training, 1-day memory after spaced training remained normal (Fig. 3, D and E, and fig. S8B).

DAL axons are structurally connected with MB calyx. Using Dscam-GFP as a dendritic marker, we showed that putative DAL dendrites distributed mainly in the superior dorsofrontal protocerebrum (SDFP) region (Fig. 3I, left). Using synaptotagmin-GFP as an axon marker, we showed that DAL axons distributed widely in three brain regions: SDFP, dorsolateral protocerebrum (DLP), and inferior dorsofrontal protocerebrum (IDFP) (Fig. 3I, right) (*15*). By a close examination of *G0431-Gal4* expression pattern in the brain counterstained with DLG-antibody immunostaining, we noticed that the DAL axons and the MB calyx intersected at K5 region where dendrites belonging to pioneer αβ neurons are aggregated (*27*). Using GFP reconstitution across synaptic partners (GRASP) labeling (*28*), we verified that DAL neurons in *G0431-Gal4* and the MB pioneer αβ neurons in *L5275-LexA* (Fig. 3J, left) were structurally interconnected at the K5 region (Fig. 3J, right).

Identification of newly synthesized proteins in DAL neurons during LTM formation. Immunostaining revealed preferential expression of DDC, PER, dNR1, dNR2, CaMKII, TEQ (TEQUILA), and CRY proteins and octopamine in DAL neurons (fig. S9A). Using RNA interference (RNAi) with *UAS-perPAS-IR G2* (*29*) driven by four different *Gal4* drivers (*per-Gal4*, *Ddc-Gal4*, *G0338-Gal4*, and *G0431-Gal4*), we found that constitutive disruption of PER protein expression impaired LTM formation after spaced training but not after massed training (Fig. 4A and fig. S9, B to D). Constitutive *UAS-perPAS-IR G2* expression in ellipsoid body neurons (*Feb170-Gal4*) did not affect 1-day memory after spaced training (fig. S9E). Similarly, expressing with *G0431-Gal4*, RNAi constructs for dNR1/dNR2, CaMKII, TEQUILA, or DDC/TRH also impaired LTM formation after spaced training but not after massed training (Fig. 4, B to E). To eliminate any developmental contribution to the impairments observed above, we repeated the same set of experiments using a temperature-sensitive tub-Gal80^{ts} protein that suppresses *Gal4*-induced expression at 18°C but not at 30°C (*30*). When *G0431-Gal4*–induced RNAi expression for *per, dNR1/dNR2, CaMKII, tequila, and Ddc/Trh* genes were suppressed throughout development (18°C) and then allowed only in adults (30°C), we again observed defects in 1-day memory after spaced but not after massed training. Moreover, in each case, further inhibition of protein synthesis from feeding flies cycloheximide did not produce stronger LTM impairments (Fig. 4, F to J).

We also found that down-regulation of CRY or overexpression of CER in DAL neurons impaired 1-day memory after spaced training after constitutive, but not after adult-specific, transgenic manipulations (fig. S9, F and G). Moreover, adult-specific *Tβh^{RNAi}* expression in DAL neurons did not affect 1-day memory after spaced training (fig. S9H).

CREB2 activity in DAL neurons, but not MB neurons, is required for LTM formation. We confirmed an earlier report that 1-day memory after spaced training was impaired, but learning was normal, after constitutive expression in MB neurons by the *c739-Gal4* driver of *UAS-dcreb2-b*, which encodes a CREB repressor protein (*4*, *7*). However, learning was impaired after constitutive expression of *UAS-dcreb2-b* by two additional

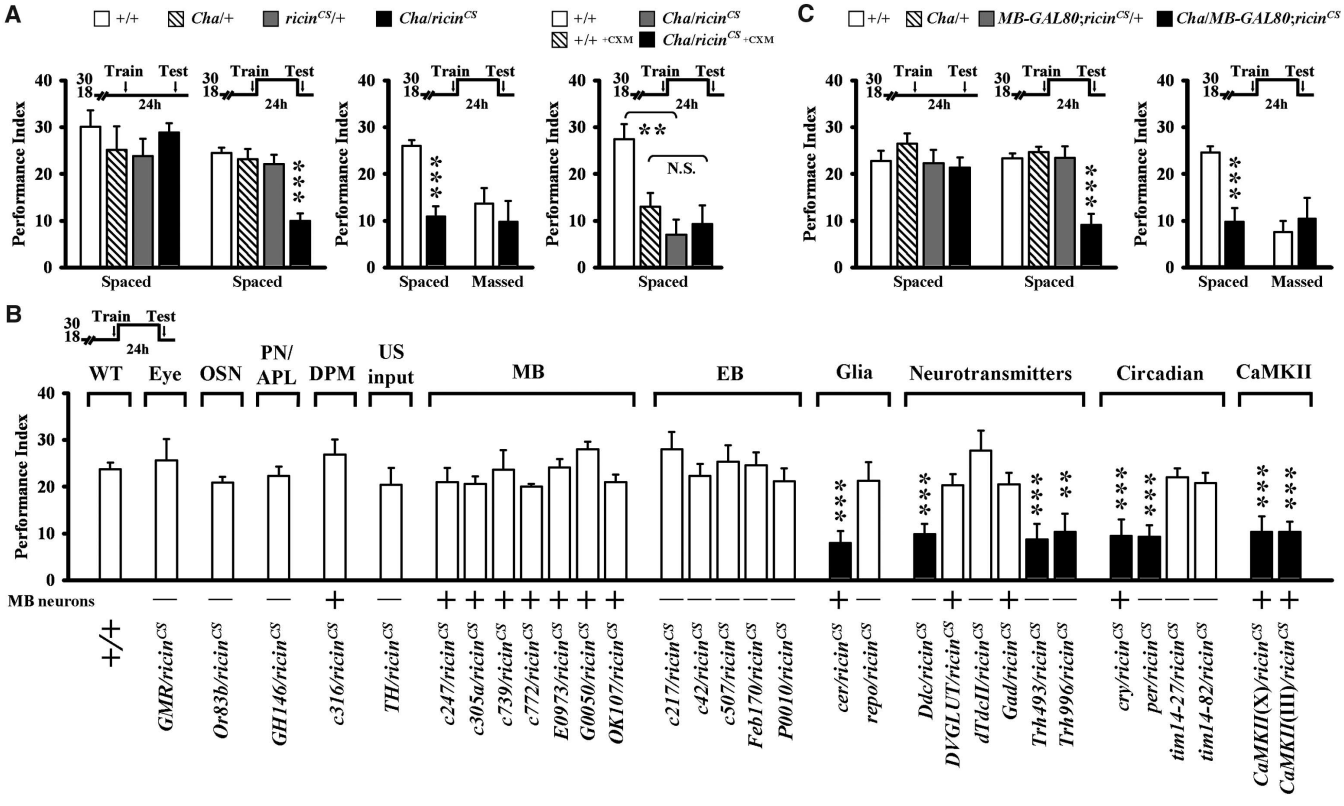

Fig. 2. Behavioral screen for neurons in which protein synthesis is required for LTM formation. (**A**) Protein synthesis is required in *Cha-Gal4* neurons for normal LTM formation. After spaced or massed training, *Cha-Gal4>UAS-ricin^{CS}* flies fed with (+) or without (–) cycloheximide (CXM) were shifted to 30°C or remained at 18°C. Values are means ± SEM (N = 12 experiments; **, $P < 0.01$; ***, $P < 0.001$; N.S., $P > 0.05$). (**B**) Behavioral screen for *Gal4* expression patterns containing neurons in which protein synthesis is required for LTM formation. All flies were subjected to spaced training, and then RICIN^{CS} was activated by keeping flies at 30°C during the 24-hour retention interval. Black bars denote significant impairments of 1-day memory. *Gal4* expression patterns containing MB neurons (+) or not (–) are indicated. Values are means ± SEM (N = 8 to 12 experiments; **, $P < 0.01$; ***, $P < 0.001$). (**C**) Protein synthesis is required for LTM formation in *Cha-Gal4*–expressing neurons outside of MB. *MB-Gal80* inhibits *Gal4* expression in the MB neurons. Values are means ± SEM (N = 12 experiments; ***, $P < 0.001$). See table S1 for a summary of *Gal4* expression patterns.

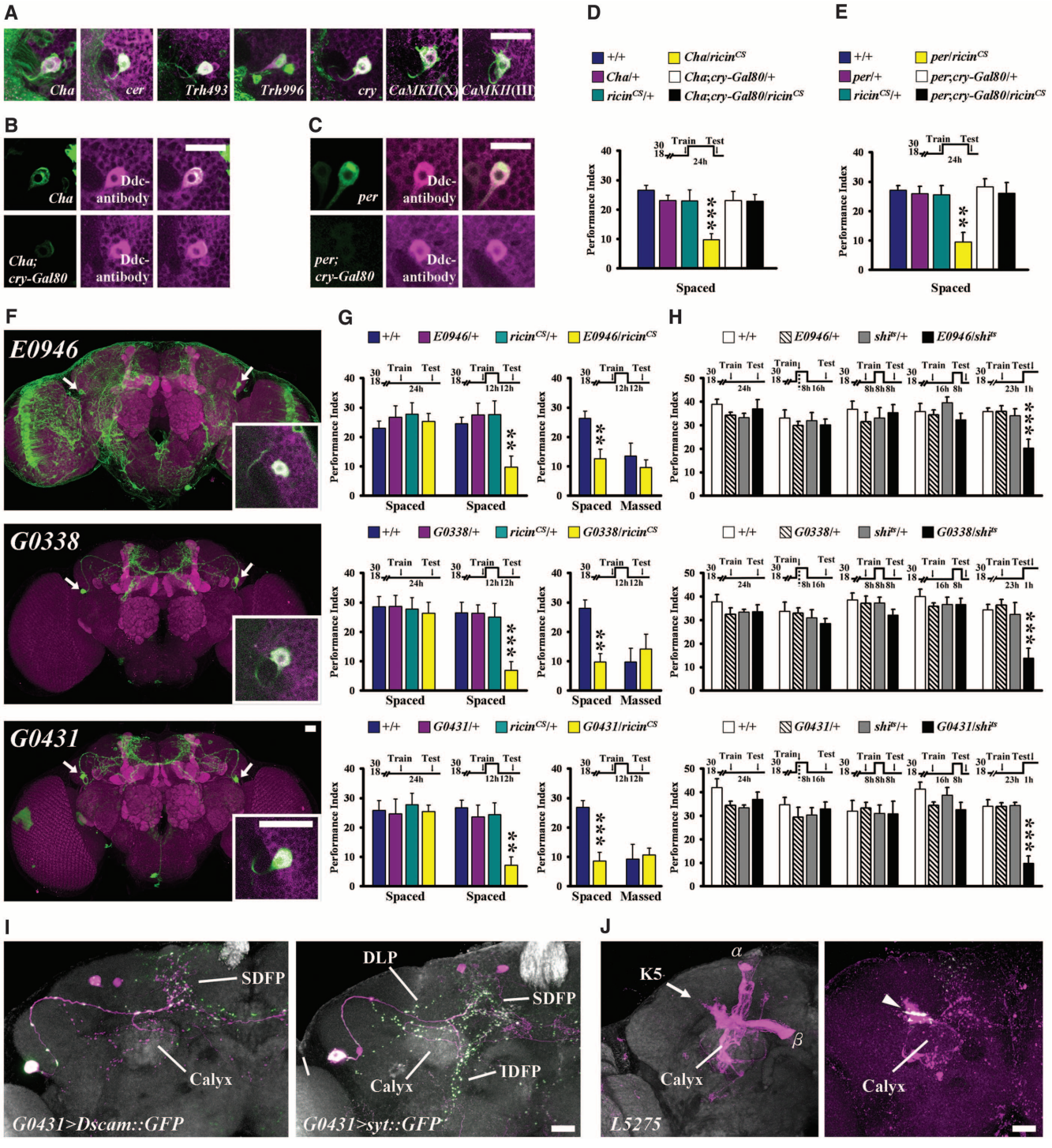

Fig. 3. DAL neurons are required for consolidation and retrieval of LTM. (**A**) The same DAL neurons contained in seven different *Gal4*, as indicated by DDC-antibody immunostaining (magenta). (**B** and **C**) DAL neurons are "subtracted" from the *Gal4* expression pattern (green) by *cry-Gal80*. (**D** and **E**) LTM formation required protein synthesis in neurons within the intersected expression between *Cha-Gal4* and *cry-Gal80* or between *per-Gal4* and *cry-Gal80*. Values are means ± SEM ($N = 12$ experiments; **, $P < 0.01$ ***, $P < 0.001$). (**F**) Three independent *Gal4* lines with more restricted expression patterns containing DAL neurons (arrow). (Inset) The identity of DAL neurons was verified using DDC-antibody immunostaining (magenta). (**G**) Protein synthesis in DAL neurons is required for LTM formation. Values are means ± SEM ($N = 8$ to 12 experiments; **, $P < 0.01$; ***, $P < 0.001$). (**H**) Neurotransmission from DAL neurons is required during LTM retrieval. One-day memory after spaced training was impaired when neurotransmission from DAL neurons was blocked (by transferring flies to 30°C for 1 hour) during the test trial (retrieval) but not during acquisition or (i) 0 to 8 hours, (ii) 8 to 16 hours, or (iii) 16 to 24 hours of the 24-hour retention interval (consolidation). Control flies kept continuously at 18°C exhibited normal 1-day memory retention. Values are means ± SEM ($N = 8$ to 12 experiments; ***, $P < 0.001$). (**I**) Polarity analysis of the DAL neuron (magenta). (Left) Putative dendrites labeled by Dscam-GFP (green). (Right) Putative axons labeled by syt-GFP (green). DLP, dorsolateral protocerebrum; IDFP, inferior dorsofrontal protocerebrum; SDFP, superior dorsofrontal protocerebrum. (**J**) Structural connections between DAL and MB neurons visualized by GRASP labeling. (Left) *L5275*-LexA expressed specifically in the MB pioneer αβ neurons. (Right) GRASP signal (arrowhead) was visualized in the K5 region. DAL and pioneer αβ neurons were labeled by CD4-antibody immunostaining (magenta). General brain structures were counterstained using DLG-antibody immunostaining [magenta in (F); grayscale in (I) and (J)]. Scale bar, 20 μm.

MB driver lines, *OK107-Gal4* and *c247-Gal4* (fig. S10, A to C). These learning defects prompted us to examine whether constitutive expression of *UAS-dcreb2-b* in MB neurons might produce any developmental defects. For all three *Gal4* driver lines, we discovered significant neuroanatomical damage in MB. In *OK107-Gal4>UAS-dcreb2-b* flies, the α′ lobe was completely missing (fig. S10D); in *c247-Gal4>UAS-dcreb2-b* or *c739-Gal4>UAS-dcreb2-b* flies, MBs had significantly fewer GFP axons compared with control flies (fig. S10, E and F), and β lobe axons occasionally crossed the midline (fig. S10F).

To eliminate these developmental defects, we used *tub-Gal80^{ts}* to limit *UAS-dcreb2-b* expression

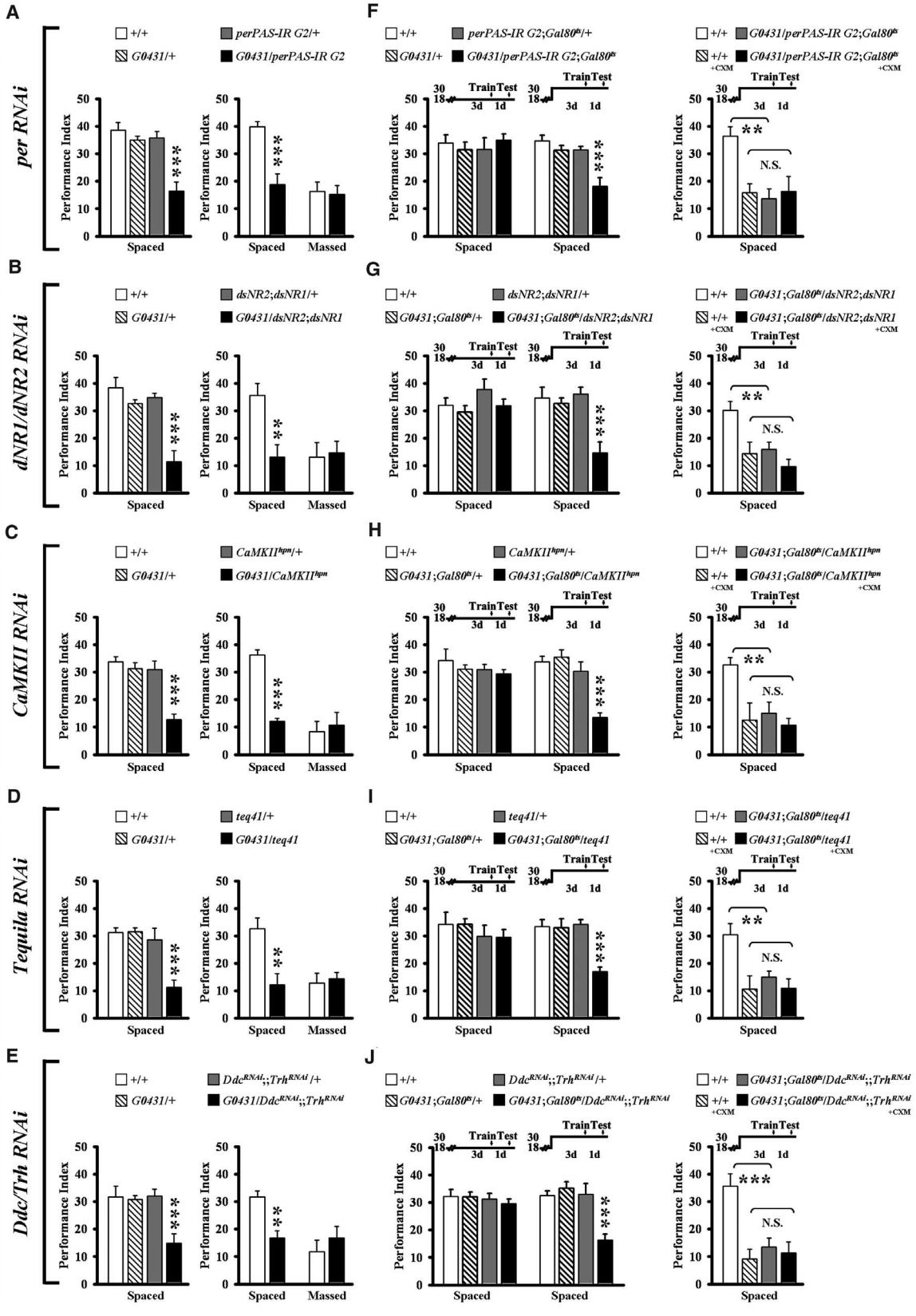

Fig. 4. RNAi-mediated disruption of specific genes in DAL neurons impairs LTM formation. (**A** to **E**) Constitutive RNAi-mediated down-regulation of PER, dNR1/dNR2, CaMKII, TEQUILA, and DDC/TRH in DAL neurons impaired 1-day memory after spaced training but not after massed training. Values are means ± SEM (N = 8 to 12 experiments; **, P < 0.01; ***, P < 0.001; N.S., P > 0.05). (**F** to **J**) Induced down-regulation of PER, dNR1/dNR2, CaMKII, TEQUILA, and DDC/TRH in the DAL neurons in adult flies impaired 1-day memory after spaced training but not after massed training. Adult flies raised at 18°C were kept at 30°C for 3 days before training to remove *tub-Gal80^{ts}*–mediated inhibition of *Gal4* activity, thereby allowing *RNAi*-mediated disruption of the target gene(s). Some groups also were fed with 35 mM cycloheximide (+CXM) 1 day before training and again until test trial. Control flies carrying the same transgenes were kept continuously at 18°C before behavioral evaluations. Values are means ± SEM (N = 8 to 12 experiments; **, P < 0.01; ***, P < 0.001; N.S., P > 0.05).

by *OK107-Gal4*, *c247-Gal4*, or *c739-Gal4* to adults (fig. S10, G to I). Under these conditions, memory retention immediately after one training session and 1-day memory after spaced training both were normal (fig. S10, J to L). MB morphology was severely damaged if these flies were kept at 30°C throughout development (fig. S10M). Note that *c739-Gal4*, but not *OK107-Gal4* or *c247-Gal4*, expressed weakly also in DAL neurons (fig. S10N). In contrast, when *UAS-dcreb2-b* expression was limited to the adult stage in *ChaGal4>UAS-dcreb2-b;tub-Gal80^{ts}* flies, 1-day memory after spaced training, but not immediate memory after one training session, was impaired (fig. S10, O and P).

Next, we asked whether CREB2 activity is required in DAL neurons during LTM formation. Adult-specific (or constitutive) overexpression of *UAS-dcreb2-b* or RNAi-mediated down-regulation of CREB2 expression in DAL neurons impaired 1-day memory after spaced training but not after massed training (Fig. 5, A to D), and feeding with cycloheximide did not exaggerate these impairments (Fig. 5, C and D).

Visualizing transcriptional activity in identified neurons during LTM formation. Thus far, we have shown that LTM formation is impaired by acute (adult-specific) disruptions of eight different genes (i.e., *per*, *dNR1*, *dNR2*, *CaMKII*, *Teq*, *Ddc*, *Trh*, and *dcreb2*) in DAL neurons (Figs. 4 and 5). Because these disruptions existed before and after training, we wanted to determine whether spaced training itself induced expression of these genes.

CaMKII-Gal4 expresses in both MB and DAL neurons (fig. S2B). LTM formation requires normal expression of CaMKII at the time of training in *CaMKII-Gal4* neurons (*19*) and in MB neurons (*7*). When activated immediately after spaced training, RICIN^{CS} in *CaMKII-Gal4* neurons impairs 1-day memory (Fig. 2B) but, in contrast, RICIN^{CS} in MB neurons does not (fig. S4). Is the synthesis of CaMKII induced by spaced training? We used KAEDE to report the transcriptional activity of *CaMKII* for a 24-hour interval after spaced (or massed) training. After photoconversion of preexisting KAEDE (red), spaced training, but not massed training, specifically induced new KAEDE (green) in DAL neurons when *UAS-kaede* was driven by *CaMKII-Gal4* (Fig. 6A). Quantification of newly synthesized green KAEDE indicated that *CaMKII* promoter activity in the DAL neurons is induced only by spaced training, because the low baseline level of green KAEDE after massed training remained constant throughout the 24-hour interval. In MB neurons, KAEDE synthesis driven by *CaMKII-Gal4* remained at a constant low level at the tip of the α lobe or the soma of the MB after either spaced or massed training (Fig. 6A). In the DAL neurons, KAEDE synthesis driven by *per-Gal4* likewise was elevated after spaced training but not after massed training (Fig. 6B). We did not see the spaced training–induced elevation of KAEDE synthesis in any other neurons contained in *CaMKII*-Gal4 and *per*-Gal4, whether imaging at the same detection sensitivity maximized for the DAL neurons or at a lower detection sensitivity maximized for the MB or the lateral circadian neurons (fig. S11). This elevation of *CaMKII* and *per* transcriptional activities occurred mainly during the first 8 hours and then gradually declined, as indicated by monitoring KAEDE synthesis in the DAL neurons in three time regimens after spaced training (fig. S12). By using *tub-Gal80^{ts}* to limit *Gal4*-driven *UAS-dcreb2-b* expression at the adult stage, we found that spaced training–induced levels of KAEDE synthesis driven by *CaMKII-Gal4* or *per-Gal4* in DAL neurons were diminished (Fig. 6C).

Three other genes, *cry*, *Ddc* and *Trh*, were not transcriptionally up-regulated after spaced or massed training, as reported by de novo KAEDE synthesis, even though their normal functions are required in DAL neurons for normal LTM formation (Fig. 6, D to F). We also evaluated an unknown gene, in which the *G0431-Gal4* enhancer trap P element is inserted. Homozygous *G0431-Gal4/G0431-Gal4* flies exhibited normal

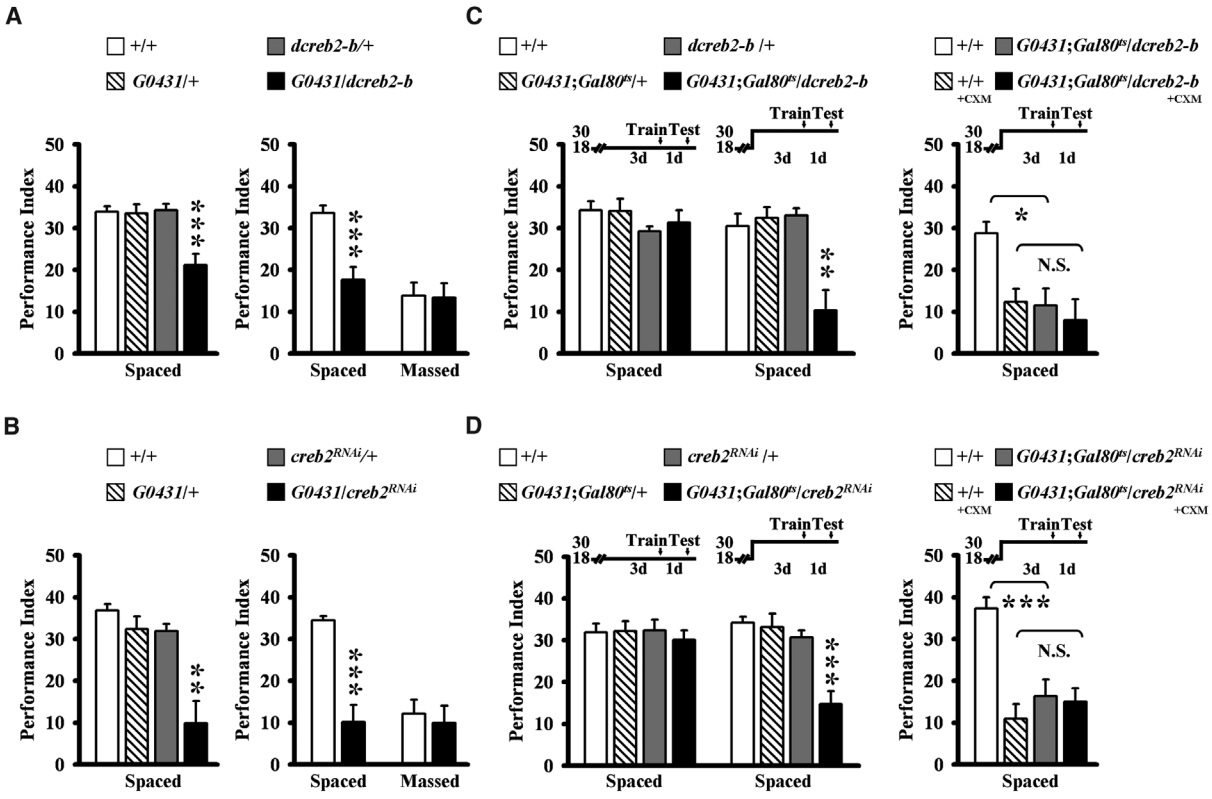

Fig. 5. CREB2 activity in DAL neurons is required for LTM formation. (**A** and **B**) Constitutive expression of *UAS-dcreb2-b* or *UAS-creb2^{RNAi}* in the *G0431-Gal4* neurons impaired 1-day memory after spaced training but not after massed training. Values are means ± SEM (N = 8 to 12 experiments; **, $P < 0.01$; ***, $P < 0.001$; N.S., $P > 0.05$). (**C** and **D**) Induced expression of *UAS-dcreb2-b* or *UAS-creb2^{RNAi}* in *G0431-Gal4* neurons impaired 1-day memory after spaced training but not after massed training. Adult flies raised at 18°C were transferred to 30°C for 3 days before training to remove *tub-Gal80^{ts}* inhibition of *Gal4* activity. Some groups also were fed with cycloheximide (+CXM) before training. One-day memory after spaced training also was evaluated for control flies carrying the same transgenes but kept continuously at 18°C. Values are means ± SEM (N = 8 to 12 experiments; *, $P < 0.05$; **, $P < 0.01$; ***, $P < 0.001$; N.S., $P > 0.05$).

1-day memory after spaced training (fig. S13). In DAL neurons of *G0431-Gal4>UAS-kaede* flies, constant low levels of KAEDE synthesis were seen throughout the 24-hour interval after spaced or massed training (fig. S13).

Discussion. We used genetically based methods to identify neurons in the *Drosophila* brain in which protein synthesis is required for LTM formation. The bilaterally paired DAL neurons satisfy several criteria to suggest that they are a site of LTM storage (*6*). First, de novo protein synthesis in DAL neurons during the first 12 hours after spaced training was required for normal LTM formation (Fig. 3G). Second, several proteins (i.e., dNR1, dNR2, PER, CaMKII, and TEQUILA) that have previously been shown to be necessary for LTM formation (*19*, *21*, *23*, *26*, *31*) were colocalized in DAL neurons (figs. S6A and S9A). Third, disruptions of PER, dNR1, dNR2, CaMKII, TEQUILA, DDC, TRH, and CREB2 in DAL neurons impaired 1-day memory after spaced (but not massed) training (Fig. 4 and Fig. 5, B and D). Fourth, expression of a repressor form of CREB2 protein in DAL neurons was sufficient

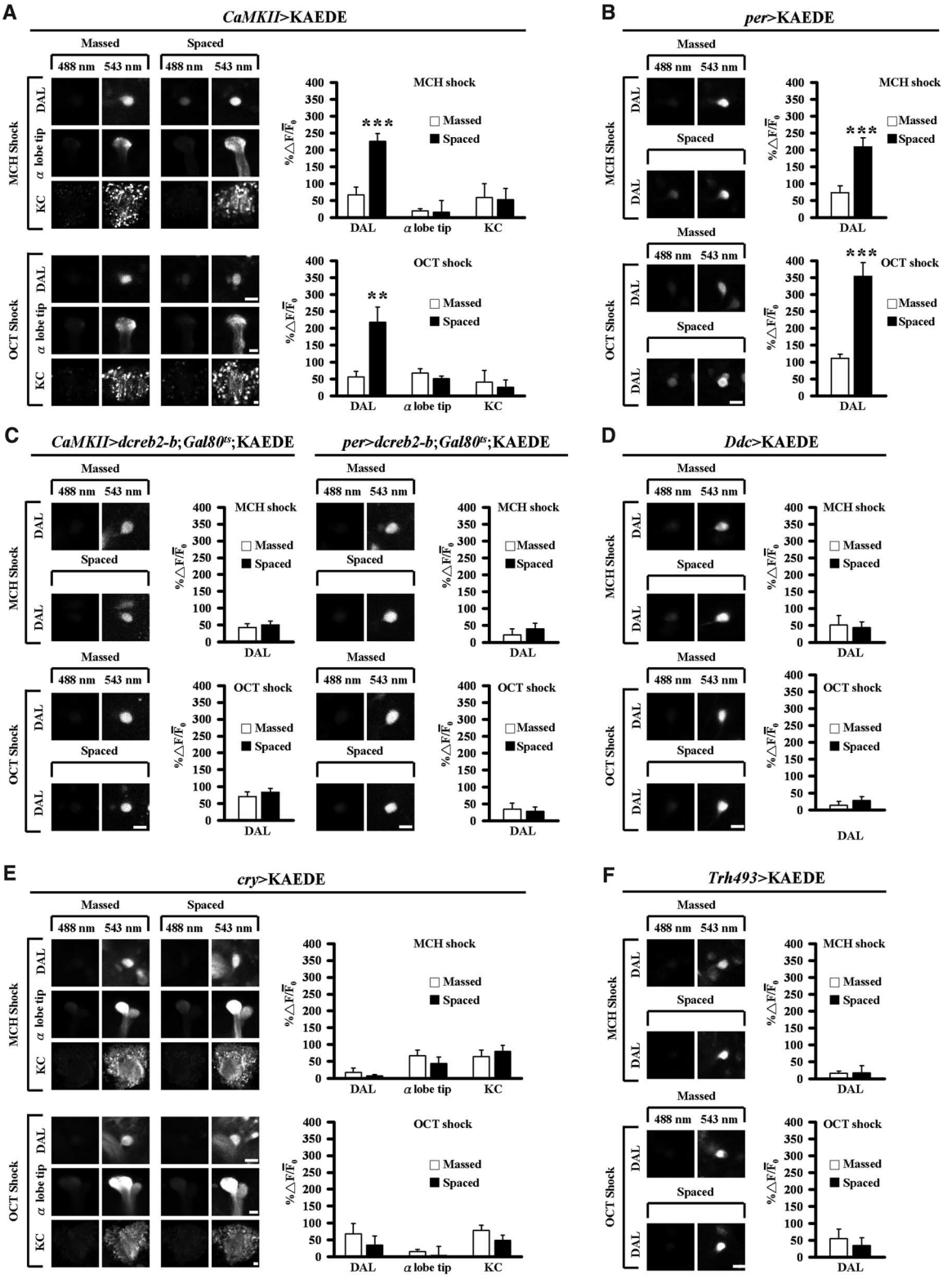

Fig. 6. (A to F) Spaced training–induced transcriptional activities. Living flies were subjected to UV irradiation to convert green KAEDE into red KAEDE just before training. KAEDE levels were quantified 24 hours after spaced or massed training to either 3-octanol (OCT) or 4-methylcyclohexanol (MCH). For each brain, a single optical slice through the cell body of a DAL neuron, MB α lobe tip, or MB cell bodies was taken under the same imaging conditions. KAEDE synthesis was determined as a ratio of new (green, 488 nm) to preexisting (red, 543 nm) KAEDE (%$\Delta F/\bar{F}_0$). Adult specific expression of *UAS-dcreb2-b* was performed by removing *tub-Gal80^{ts}* inhibition at 30°C for 3 days before the experiment. Values are means ± SEM (N = 8 to 24 samples; **, $P < 0.01$; ***, $P < 0.001$). Scale bar, 10 μm.

to disrupt 1-day memory after spaced (but not massed) training (Fig. 5, A and C). Fifth, the transcriptional activities of *CaMKII* and *per* were elevated in DAL neurons after spaced (but not massed) training (Fig. 6, A and B). Sixth, the up-regulations of *CaMKII* and *per* in DAL neurons were CREB2-dependent (Fig. 6C). Seventh, neurotransmission from DAL neurons was required only for LTM retrieval but not for acquisition (LRN) or consolidation of LTM (Fig. 3H and fig. S7). Together, these data suggest that CaMKII and PER are bona fide "LTM proteins" synthesized in DAL neurons after spaced training.

RICIN^{CS} not only allowed us to target inhibition of protein synthesis to individual neurons but also allowed us to investigate the critical window for protein synthesis during LTM formation, because of its rapid temporal control (Fig. 1C). Unexpectedly, activated RICIN^{CS} did not affect LTM formation when expressed in MB neurons (Fig. 2B and fig. S5). Previous studies have shown that LTM formation involves the vertical axonal branches of αβ neurons in MBs (*20*), and LTM formation is blocked by overexpression of CREB repressor in MB [using *c739-Gal4* (*4*)]. Moreover, increases in neural activity in these structures at the time of LTM retrieval appear CREB-dependent (*4*, *7*). We clarified this apparent discrepancy by showing that (i) constitutive expression of CREB2b or RICIN^{CS} in the MB neurons (using *c739-Gal4*, *OK107-Gal4*, and *c247-Gal4*) resulted in developmental defects of MB structure, along with defects in LTM (figs. S1 and S10); (ii) adult stage–restricted expression of CREB2b or activated RICIN^{CS} in MB neurons yielded no detectable structural defects of MB and no LTM defects (figs. S5 and S10); (iii) adult stage–restricted expression of CREB2b or activated RICIN^{CS} in DAL neurons was sufficient to impair LTM formation (Figs. 3 and 5); and (iv) spaced training–induced elevation of CaMKII occurred in DAL neurons but not in MB neurons and was diminished by expression of CREB2b (Fig. 6).

Possibly, a more stringent requirement for inhibition of protein synthesis exists in MB neurons rather than in DAL neurons. A 50% reduction of total protein synthesis in fly brains from cycloheximide feeding is sufficient to block LTM formation (*1*). Here, we show that activated RICIN^{CS} in MB (or *per*-expressing) neurons results in an 80% reduction of KAEDE synthesis (Fig. 1, C to E). Also worth noting is that LTM defects in *dFmr1* mutants can be ameliorated somewhat by feeding flies inhibitors of protein synthesis (*32*). Thus, the inhibition of negative regulators of genes involved in LTM formation (in MB neurons) theoretically could enhance, rather than impair, 1-day memory after spaced training—an outcome we did not monitor in this study.

A functional memory circuit must (i) register (acquire) an experience through a persistent neural activity, (ii) consolidate (store) a lasting memory through (protein synthesis–dependent) structural or functional changes somewhere in that circuit; and (iii) retrieve a long-term memory through reactivation of (some or all) of the circuit. Neural activity in MB neurons contributes to acquisition, consolidation, and retrieval of LTM (*3*, *8*, *20*, *21*, *33*, *34*). Indeed, more than 30 different disruptions of LTM formation also diminish the calcium-based neural activity observed in αβ neurons in MB (*3*, *8*). Importantly, expression patterns of many genes involved in LTM formation suggest that other neuroanatomical regions also participate in neural activity essential for LTM formation, including glial cells (*35*), antenna lobes (*19*), asymmetrical body (*36*), ellipsoid body (*21*), many other unidentified neurons in 17 different LTM mutants (*37*), and, of course, DAL neurons. The latter are an interesting case, because neurotransmission from DAL neurons appears to be required only for retrieval, but not for acquisition or consolidation, of LTM (Fig. 3 and fig. S7). None of these data are sufficient, however, to identify the neurons in which protein synthesis–dependent memory consolidation (storage) occurs.

We provide evidence of memory consolidation in identified neurons via the combination of direct observation of protein synthesis with disruption of LTM formation through targeted inhibition of protein synthesis by activated RICIN^{CS}. We also found a CREB2-dependent up-regulation of CaMKII and PER after spaced but not massed training (Fig. 6, A to C), only the former of which induces LTM formation. These observations support the hypothesis that LTM consolidation occurs, at least in part, through CREB-mediated modulation of gene expression in DAL neurons (*2*, *38*). Further, our results indicate that CaMKII, PER, CREB2, DDC, TRH, dNR1, dNR2 and TEQUILA in DAL neurons are required at the time of training for normal LTM formation. In the case of DDC and TRH, however, spaced training did not up-regulate their transcription (Fig. 6, C to E), so they either are regulated posttranscriptionally or function as "basal" cellular machinery for the consolidation process.

Our data suggest a MB-DAL loop as part of the olfactory memory circuit. An olfactory experience first is communicated through olfactory sensory neurons and antennal lobe and registered in MB-APL-DPM as a neural activity (*19*, *39*–*42*). Neurotransmission from MB to DAL for consolidation (MB to DAL) occurs, and protein synthesis within DAL then yields structural and/or functional changes in DAL neural activity that communicate back to MB during retrieval (DAL to MB). Our observation that activated RICIN^{CS} in neurons of the *cer-Gal4* expression pattern other than DAL still impairs LTM formation suggests that other extra-MB neurons also participate in the consolidation of LTM.

References and Notes

1. T. Tully, T. Préat, S. C. Boynton, M. Del Vecchio, *Cell* **79**, 35 (1994).
2. J. C. Yin *et al.*, *Cell* **79**, 49 (1994).
3. R. L. Davis, *Neuron* **70**, 8 (2011).
4. D. Yu, D. B. Akalal, R. L. Davis, *Neuron* **52**, 845 (2006).
5. M. Heisenberg, *Nat. Rev. Neurosci.* **4**, 266 (2003).
6. B. Gerber, H. Tanimoto, M. Heisenberg, *Curr. Opin. Neurobiol.* **14**, 737 (2004).
7. D. B. Akalal, D. Yu, R. L. Davis, *J. Neurosci.* **30**, 16699 (2010).
8. D. B. Akalal, D. Yu, R. L. Davis, *J. Neurosci.* **31**, 5643 (2011).
9. R. Ando, H. Hama, M. Yamamoto-Hino, H. Mizuno, A. Miyawaki, *Proc. Natl. Acad. Sci. U.S.A.* **99**, 12651 (2002).
10. H. Mizuno *et al.*, *Mol. Cell* **12**, 1051 (2003).
11. P. E. Hardin, J. C. Hall, M. Rosbash, *Nature* **343**, 536 (1990).
12. Y. Endo, K. Mitsui, M. Motizuki, K. Tsurugi, *J. Biol. Chem.* **262**, 5908 (1987).
13. Y. Endo, K. Tsurugi, *J. Biol. Chem.* **262**, 8128 (1987).
14. K. G. Moffat, J. H. Gould, H. K. Smith, C. J. O'Kane, *Development* **114**, 681 (1992).
15. A. S. Chiang *et al.*, *Curr. Biol.* **21**, 1 (2011).
16. T. Riemensperger, T. Völler, P. Stock, E. Buchner, A. Fiala, *Curr. Biol.* **15**, 1953 (2005).
17. A. Claridge-Chang *et al.*, *Cell* **139**, 405 (2009).
18. Y. Aso *et al.*, *Curr. Biol.* **20**, 1445 (2010).
19. S. I. Ashraf, A. L. McLoon, S. M. Sclarsic, S. Kunes, *Cell* **124**, 191 (2006).
20. A. Pascual, T. Préat, *Science* **294**, 1115 (2001).
21. C. L. Wu *et al.*, *Nat. Neurosci.* **10**, 1578 (2007).
22. M. P. Belvin, H. Zhou, J. C. Yin, *Neuron* **22**, 777 (1999).
23. T. Sakai, T. Tamura, T. Kitamoto, Y. Kidokoro, *Proc. Natl. Acad. Sci. U.S.A.* **101**, 16058 (2004).
24. J. Dubnau, L. Grady, T. Kitamoto, T. Tully, *Nature* **411**, 476 (2001).
25. S. E. McGuire, P. T. Le, R. L. Davis, *Science* **293**, 1330 (2001).
26. S. Xia *et al.*, *Curr. Biol.* **15**, 603 (2005).
27. H. H. Lin, J. S. Lai, A. L. Chin, Y. C. Chen, A. S. Chiang, *Cell* **128**, 1205 (2007).
28. M. D. Gordon, K. Scott, *Neuron* **61**, 373 (2009).
29. S. Martinek, M. W. Young, *Genetics* **156**, 1717 (2000).
30. S. E. McGuire, P. T. Le, A. J. Osborn, K. Matsumoto, R. L. Davis, *Science* **302**, 1765 (2003).
31. G. Didelot *et al.*, *Science* **313**, 851 (2006).
32. F. V. Bolduc, K. Bell, H. Cox, K. S. Broadie, T. Tully, *Nat. Neurosci.* **11**, 1143 (2008).
33. G. Isabel, A. Pascual, T. Préat, *Science* **304**, 1024 (2004).
34. J. Séjourné *et al.*, *Nat. Neurosci.* **14**, 903 (2011).
35. D. Comas, F. Petit, T. Préat, *Nature* **430**, 460 (2004).
36. A. Pascual, K. L. Huang, J. Neveu, T. Préat, *Nature* **427**, 605 (2004).
37. J. Dubnau *et al.*, *Curr. Biol.* **13**, 286 (2003).
38. R. Bourtchuladze *et al.*, *Cell* **79**, 59 (1994).
39. A. C. Keene, S. Waddell, *Nat. Rev. Neurosci.* **8**, 341 (2007).
40. X. Liu, R. L. Davis, *Nat. Neurosci.* **12**, 53 (2009).
41. C. L. Wu *et al.*, *Curr. Biol.* **21**, 848 (2011).
42. J. L. Pitman *et al.*, *Curr. Biol.* **21**, 855 (2011).

Acknowledgments: We thank S. Benzer, J. Blau, R. L. Davis, J. Hall, J. Hirsh, C. J. O'Kane, S. Kunes, L. Luo, T. Préat, M. Rosbash, S. Waddell, Y. Takamatsu, M. W. Young, and the Bloomington and Drosophila Genomics Resource Centers for fly stocks. We thank J. Hirsh, L. C. Griffith, and T. Préat for the antibodies. We also thank S. F. Teng for the preliminary test of *UAS-kaede*. This work was funded by grants from Dart Neurosciences LLC, National Science Council, and Ministry of Education to A.-S.C. C.-C.C., T.T., and A.-S.C. conceptualized the project and wrote the manuscript; C.-C.C. and A.-S.C. developed the methods and analyzed the data; C.-C.C., J.-K.W., T.-P.P., and C.-L.W carried out behavioral experiments; H.-W.L. and J.-K.W. performed imaging experiments; T.-F.F. generated the *UAS-kaede* transgenic flies; A.-S.C. supervised the project. The authors declare no competing financial interests. Correspondence and requests for materials should be addressed to A.-S.C.

Supporting Online Material

www.sciencemag.org/cgi/content/full/335/6069/678/DC1
Materials and Methods
Figs. S1 to S13
References (*43*–*45*)
Movie S1

16 August 2011; accepted 2 December 2011
10.1126/science.1212735

www.sciencemag.org/cgi/content/full/335/6069/678/DC1

Supporting Online Material for

Visualizing Long-Term Memory Formation in Two Neurons of the *Drosophila* Brain

Chun-Chao Chen, Jie-Kai Wu, Hsuan-Wen Lin, Tsung-Pin Pai,
Tsai-Feng Fu, Chia-Lin Wu, Tim Tully, Ann-Shyn Chiang*

*To whom correspondence should be addressed. E-mail: aschiang@life.nthu.edu.tw

Published 10 February 2012, *Science* **335**, 678 (2012)
DOI: 10.1126/science.1212735

This PDF file includes:

Other Supporting Online Material for this manuscript includes the following:
(available at www.sciencemag.org/cgi/content/full/335/6069/678/DC1)

Supporting Online Material

Supporting figure legends

Fig. 1. Visualizing and blocking *de novo* protein synthesis in identified neurons.

(**A**) A single optical section through cell bodies of lateral neurons was taken 4 hours or 12 hours after UV irradiation. Genotype: *per-Gal4*/+;*UAS-kaede*/+.

(**B**) Flies were fed 5% glucose with or without 35mM cycloheximide (CXM) for 1 day before the experiment. Genotype: *per-Gal4*/+;*UAS-kaede*/+.

(**C**) Genotype: *per-Gal4*/+;*UAS-kaede*/*UAS-ricin*^{CS}.

(**D**) For each brain sample, a single optical section through the Kenyon cell body layer was imaged under the same conditions. Genotypes: 1) *Cha-Gal4*/+;*UAS-kaede*/**+** and 2) *Cha-Gal4*/+;*UAS-kaede*,*UAS-ricin*^{CS}**/+.**

(E) For each brain sample, a single optical section through the Kenyon cell body layer was imaged under the same conditions. Genotypes: 1) *UAS-kaede*/+;*OK107-Gal4*/+ and 2) *UAS-kaede*,*UAS-ricin*^{CS}/+;*OK107-Gal4*/+**.**

Fig. 2. Behavioral screen for neurons in which protein synthesis is required for LTM formation.

(**A**) Flies were raised at 18^{o}C. 1-day memory retention was quantified at 18^{o}C. Genotypes: 1) +/+ (wild type), 2) *Cha-Gal4*/+, 3) *UAS-ricin*^{CS}/+ and 4) *Cha-Gal4*/+;*UAS-ricin*^{CS}/+.

(**B**) Genotypes: 1) +/+, 2) *GMR-Gal4*/+;*UAS-ricin*^{CS}/+, 3) *Or83b-Gal4*/+;;*UAS-ricin*^{CS}/+, 4) *GH146-Gal4*/+;*UAS-ricin*^{CS}/+, 5) *c316-Gal4*/*UAS-ricin*^{CS}, 6) *TH-Gal4*/*UAS-ricin*^{CS}, 7) *c247-Gal4*/*UAS-ricin*^{CS}, 8) *c305a-Gal4*/+;*UAS-ricin*^{CS}/+, 9) *c739-Gal4*/+;*UAS-ricin*^{CS}/+, 10) *c772-Gal4*/+;*UAS-ricin*^{CS}/+, 11) *E0973-Gal4*/+;;*UAS-ricin*^{CS}/+, 12) *G0050-Gal4*/+;;*UAS-ricin*^{CS}/+, 13) *UAS-ricin*^{CS}/+;*OK107-Gal4*/+, 14) *c217-Gal4*/+;*UAS-ricin*^{CS}/+, 15) *c42-Gal4*/*UAS-ricin*^{CS}, 16) *c507-Gal4*/*UAS-ricin*^{CS}, 17) *Feb170-Gal4*/+;*UAS-ricin*^{CS}/+, 18) *P0010-Gal4*/+;*UAS-ricin*^{CS}/+, 19) *cer-Gal4*/+;*UAS-ricin*^{CS}/+, 20) *repo*/*UAS-ricin*^{CS}, 21) *Ddc-Gal4*/+;;*UAS-ricin*^{CS}/+, 22) *DVGLUT-Gal4*/+;;*UAS-ricin*^{CS}/+, 23) *dTdcII-Gal4*/+;*UAS-ricin*^{CS}/+, 24) *Gad-Gal4*/+;*UAS-ricin*^{CS}/+, 25) *Trh493-Gal4*/*UAS-ricin*^{CS}, 26) *Trh996-Gal4*/+;;*UAS-ricin*^{CS}/+, 27) *cry-Gal4*/*UAS-ricin*^{CS}, 28) *per-Gal4*/+;*UAS-ricin*^{CS}/+, 29) *tim14-27-Gal4*/+;*UAS-ricin*^{CS}/+, 30) *tim14-82-Gal4*/+;*UAS-ricin*^{CS}/+, 31) *CaMKII-Gal4*(X)/+;;*UAS-ricin*^{CS}/+ and 32) *CaMKII-Gal4*(III)/*UAS-ricin*^{CS}.

(**C**) The experimental procedures were the same as in (**A**). Genotypes: 1) +/+, 2) *Cha-Gal4*/+, 3) *MB-Gal80*/+;*UAS-ricin*^{CS}/+ and 4) *Cha-Gal4*/*MB-Gal80*;*UAS-ricin*^{CS}/+.

Fig. 3. DAL neurons are required for consolidation and retrieval of LTM.

(**A**) *Gal4* expression patterns were labeled by the *UAS-mCD8::GFP* reporter (green). Some flies were fed with 35mM cycloheximide (+CXM), 1 day before training and again until test trial. Genotypes: 1)

Cha-Gal4/*UAS-mCD8::GFP*;*UAS-mCD8::GFP*/+, 2) *cer-Gal4*/*UAS-mCD8::GFP*;*UAS-mCD8::GFP*/+, 3) *UAS-mCD8::GFP*/+;*Trh493-Gal4*(III)/*UAS-mCD8::GFP*, 4) *Trh996-Gal4*/+;*UAS-mCD8::GFP*/+; *UAS-mCD8::GFP*/+, 5) *UAS-mCD8::GFP*/+;*cry-Gal4*/*UAS-mCD8::GFP*, 6) *CaMKII-Gal4*(X)/+; *UAS-mCD8::GFP*/+;*UAS-mCD8::GFP*/+ and 7) *UAS-mCD8::GFP*/+; *CaMKII-Gal4*(III)/*UAS-mCD8::GFP*.

(**B**) Genotypes: 1) *Cha-Gal4*/*UAS-mCD8::GFP*;*UAS-mCD8::GFP*/+ and 2) *Cha-Gal4*/*UAS-mCD8::GFP*; *cry-Gal80*/*UAS-mCD8::GFP*.

(**C**) Genotypes: 1) *per-Gal4*/*UAS-mCD8::GFP*;*UAS-mCD8::GFP*/+ and 2) *per-Gal4*/*UAS-mCD8::GFP*; *cry-Gal80*/*UAS-mCD8::GFP*.

(**D**) RICIN^{CS} was activated immediately after training and then for the 24 hour retention interval. Genotypes: 1) +/+, 2) *Cha-Gal4*/+, 3) +/*UAS-ricin*^{CS}, 4) *Cha-Gal4*/+;*UAS-ricin*^{CS}/+, 5) *Cha-Gal4*/+;*cry-Gal80*/+ and 6) *Cha-Gal4*/+;*cry-Gal80*/*UAS-ricin*^{CS}**.**

(**E**) RICIN^{CS} was activated immediately after training and then for the 24 hour retention interval. Genotypes: 1) +/+, 2) *per-Gal4*/+, 3) +/*UAS-ricin*^{CS}, 4) *per-Gal4*/+;*UAS-ricin*^{CS}/+, 5) *per-Gal4*/+;*cry-Gal80*/+ and 6) *per-Gal4*/+;*cry-Gal80*/*UAS-ricin*^{CS}**.**

(**F**) Genotypes: 1) *UAS-mCD8::GFP*/+;*E0946-Gal4*/*UAS-mCD8::GFP*, 2) *G0338-Gal4*/+;*UAS-mCD8::GFP*/+; *UAS-mCD8::GFP*/+ and 3) *G0431-Gal4*/*UAS-mCD8::GFP*;*UAS-mCD8::GFP*/+**.**

(**G**) RICIN^{CS} was activated by transferring flies to 30^{o}C immediately after training for 12 hours before evaluating 1-day memory retention. Genotypes: 1) +/+, 2) *UAS-ricin*^{CS}/+, 3) *E0946-Gal4*/+, 4) *E0946-Gal4*/*UAS-ricin*^{CS}, 5) *G0338-Gal4*/+, 6) *G0338-Gal4*/+;;*UAS-ricin*^{CS}/+, 7) *G0431-Gal4*/+ and 8) *G0431-Gal4*/+;*UAS-ricin*^{CS}/+.

(**H**) Genotypes: 1) +/+, 2) *UAS-shi*^{ts}/+, 3) *E0946-Gal4*/+, 4) *E0946-Gal4*/*UAS-shi*^{ts}, 5) *G0338-Gal4*/+, 6) *G0338-Gal4*/+;;*UAS-shi*^{ts}/+, 7) *G0431-Gal4*/+ and 8) *G0431-Gal4*/+;*UAS-shi*^{ts}/+.

(**I**) Genotypes: 1) *UAS-Dscam::GFP*/+; *G0431-Gal4*/*UAS-mKO*,*UAS-mKO* and 2) *UAS-syt::GFP*/+; *G0431-Gal4*/*UAS-mKO*,*UAS-mKO*.

(**J**) Genotype: 1) *L5275-LexA*/+;*lexAop-rCD2::GFP*/+ and 2) *G0431-Gal4*/*L5275-LexA*; *UAS-CD4::GFP*$_{1\text{-}10}$,*lexAop-CD4::GFP*$_{11}$/+.

Fig. 4. RNAi-mediated disruption of specific genes in DAL neurons impairs LTM formation.

(**A**) Genotypes: 1) +/+, 2) *G0431-Gal4*/+, 3) *UAS-perPAS-IR G2*/+ and 4) *G0431-Gal4*/*UAS-perPAS-IR G2*.

(**B**) Genotypes: 1) +/+, 2) *G0431-Gal4*/+, 3) *UAS-dsNR2*;*dsNR1*/+ and 4) *G0431-Gal4*/*UAS-dsNR2*; *UAS-dsNR1*/+.

(**C**) Genotypes: 1) +/+, 2) *G0431-Gal4*/+, 3) *UAS-CaMKII*^{hpn}/+ and 4) *G0431-Gal4*/+;*UAS-CaMKII*^{hpn}/+.

(**D**) Genotypes: 1) +/+, 2) *G0431-Gal4*/+, 3) *UAS-teq41*/+ and 4) *G0431-Gal4*/+;*UAS-teq41*/+.

(**E**) Genotypes: 1) +/+, 2) *G0431-Gal4*/+, 3) *UAS-Ddc*^{RNAi}/+;;*UAS-Trh*^{RNAi}/+ and 4) *UAS-Ddc*^{RNAi}/+; *G0431-Gal4*/+;*UAS-Trh*^{RNAi}/+.

(**F**) Genotypes: 1) +/+, 2) *G0431-Gal4*/+, 3) *UAS-perPAS-IR G2*/+;*tub-Gal80^{ts}*/+ and 4) *G0431-Gal4*/*UAS-perPAS-IR G2*;*tub-Gal80^{ts}*/+.

(**G**) Genotypes: 1) +/+, 2) *G0431-Gal4*/+;*tub-Gal80^{ts}*/+, 3) *UAS-dsNR2*/+;*UAS-dsNR1*/+ and 4) *G0431-Gal4*/*UAS-dsNR2*;*UAS-dsNR1*/*tub-Gal80^{ts}*.

(**H**) Genotypes: 1) +/+, 2) *G0431-Gal4*/+;*tub-Gal80^{ts}*/+, 3) *UAS-CaMKII^{hpn}*/+ and 4) *G0431-Gal4*/+;*UAS-CaMKII^{hpn}*/*tub-Gal80^{ts}*.

(**I**) Genotypes: 1) +/+, 2) *G0431-Gal4*/+;*tub-Gal80^{ts}*/+, 3) *UAS-teq41*/+ and 4) *G0431-Gal4*/+; *UAS-teq41*/*tub-Gal80^{ts}* .

(**J**) Genotypes: 1) +/+, 2) *G0431-Gal4*/+;*tub-Gal80^{ts}*/+, 3) *UAS-Ddc^{RNAi}*/+;;*UAS-Trh^{RNAi}*/+, and 4) *UAS-Ddc^{RNAi}*/+;*G0431-Gal4*/+;*UAS-Trh^{RNAi}*/*tub-Gal80^{ts}*.

Fig. 5. CREB2 activity in DAL neurons is required for LTM formation.

(**A)** Genotypes: 1) +/+, 2) *G0431-Gal4*/+, 3) *UAS-dcreb2-b*/+ and 4) *UAS-dcreb2-b*/+;*G0431-Gal4*/+.

(**B**) Genotypes: 1) +/+, 2) *G0431-Gal4*/+, 3) *UAS-creb2^{RNAi}*/+ and 4) *G0431-Gal4*/*UAS-creb2^{RNAi}*.

(**C**) Genotypes: 1) +/+, 2) *G0431-Gal4*/+;*tub-Gal80^{ts}*/+, 3) *UAS-dcreb2-b*/+ and 4) *UAS-dcreb2-b*/+;*G0431-Gal4*/+;*tub-Gal80^{ts}*/+.

(**D**) Genotypes: 1) +/+, 2) *G0431-Gal4*/+;*tub-Gal80^{ts}*/+, 3) *UAS-creb2^{RNAi}*/+ and 4) *G0431-Gal4*/*UAS-creb2^{RNAi}*;*tub-Gal80^{ts}*/+.

Fig. 6. Spaced training-induced transcriptional activities.

(**A**) Genotype: *UAS-kaede,UAS-kaede*/+;*CaMKII-Gal4*(III)/*UAS-kaede*.

(**B**) Genotype: *per-Gal4*/*UAS-kaede,UAS-kaede*;*UAS-kaede*/+.

(**C**) Genotypes: 1) *UAS-dcreb2-b*/+;*tub-Gal80^{ts}*/+;*CaMKII-Gal4*(III)/*UAS-kaede* and 2) *UAS-dcreb2-b*/+;*per-Gal4*/*tub-Gal80^{ts}*;*UAS-kaede*/+.

(**D**) Genotype: *Ddc-Gal4*/+;*UAS-kaede,UAS-kaede*/+;*UAS-kaede*/+.

(**E**) Genotype: *UAS-kaede,UAS-kaede*/+;*cry-Gal4*/*UAS-kaede.*

(**F**) Genotype: *UAS-kaede,UAS-kaede*/+;*Trh493-Gal4*/*UAS-kaede*.

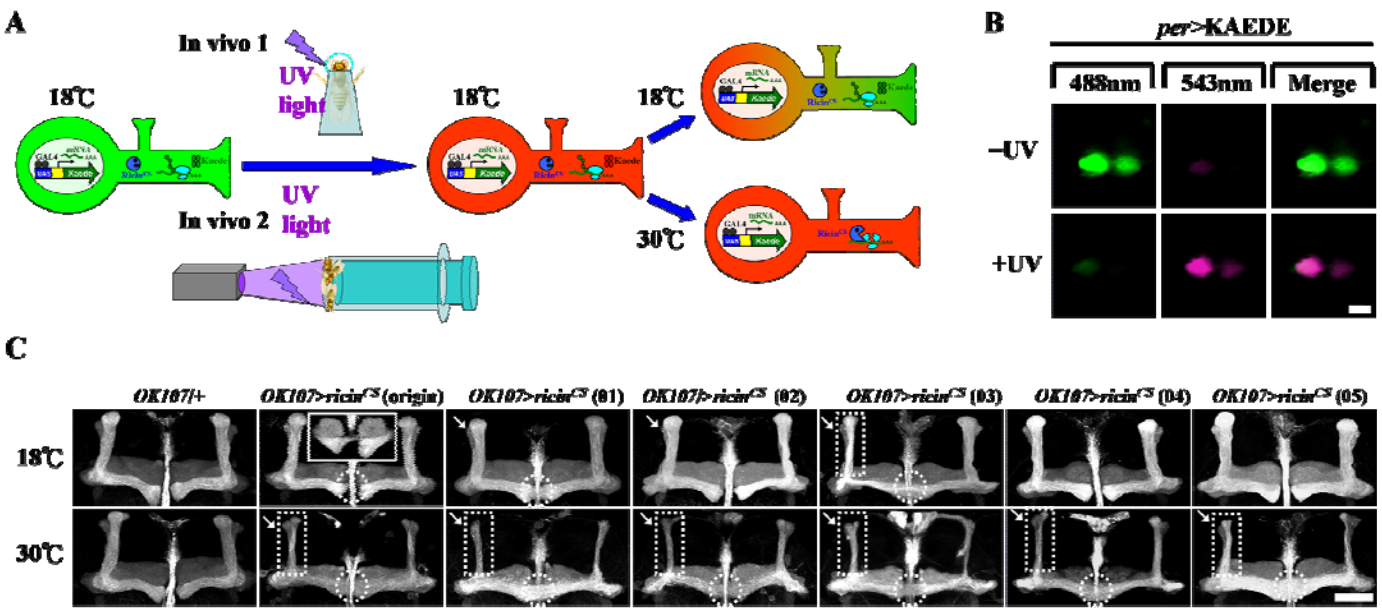

fig. S1. Characterization of *UAS-ricin*^{CS} and *UAS-kaede*. (**A**) Three schematic steps for monitoring *de novo* KAEDE synthesis in a single neuron. In flies raised at 18°C, KAEDE is a green fluorescence protein and RICIN^{CS} is inactive (left). After UV irradiation, KAEDE protein is irreversibly photoconverted into red fluorescence proteins (middle). In flies kept at 18°C after photoconversion, RICIN^{CS} is inactive and new green KAEDE is synthesized and accumulates with time, while the level of pre-existing red KAEDE remains unchanged. In flies kept at 30°C after photoconversion, activated RICIN^{CS} block the synthesis of new proteins. Consequently, new green KAEDE is not synthesized, and only red KAEDE is observed in neurons (right). (**B**) KAEDE photoconversion. Before UV irradiation (-UV), KAEDE expressed in *per* neurons emits strong green fluorescence (excited by 488nm laser) and weak red fluorescence (magenta) (excited by 543nm laser). Immediately after UV irradiation (+UV), *per*>KAEDE switches to emit strong red fluorescence and weak green fluorescence. Scale bar: 10 μm. Genotype: *per-Gal4*/+;*UAS-kaede*/+. (**C**) Effects of constitutive *UAS-ricin*^{CS} expression on MB development in flies raised at 18°C or 30°C. Five *UAS-ricin*^{CS} lines (01-05) were obtained from remobilization of a previously generated *UAS-ricin*^{CS} P element transposon (original) inserted on the third chromosome (*43*). In *OK107-Gal4>UAS-ricin*^{CS} flies, leaky activity of RICIN^{CS} at low temperature resulted in deformed MBs were noticed in the original strain and new strains of 01-03. Two types of MB defects are noticed: axons crossing the midline (circles and inset) and reduced number of vertical axons (square) compared to those in control flies (*OK107/+*). In some severe cases, the α' lobe was missing (arrow). *UAS-ricin*^{CS} strains (04 and 05) did not show any defects in MB morphology at 18°C but did show severe MB defects at 30°C. *UAS-ricin*^{CS} strain (04) was used in the rest of this study. Scale bar, 50μm.

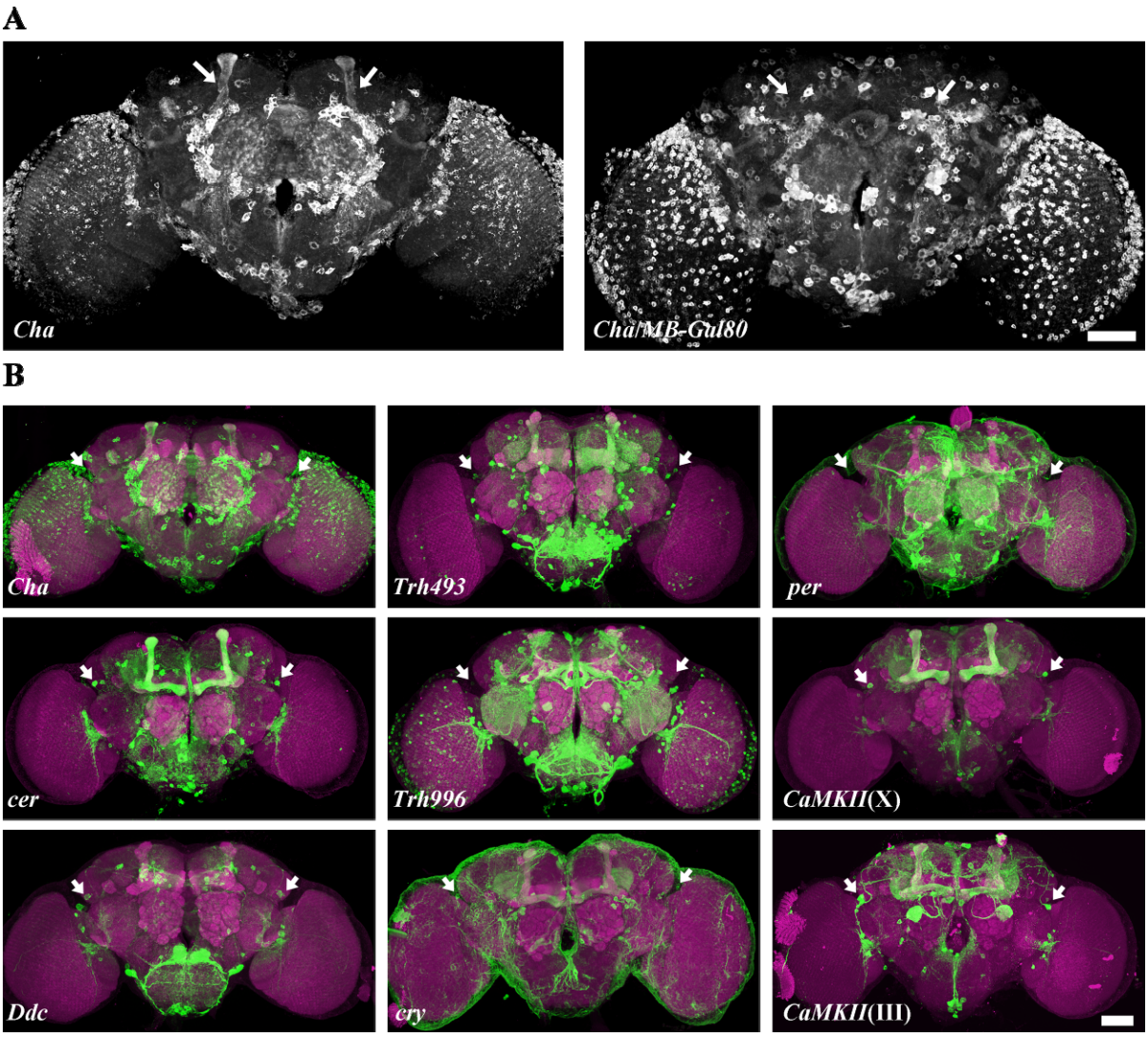

fig. S2. Expression patterns of *Gal4* drivers used for the behavioral screen in Fig. 2. (**A**) Expression patterns of *Cha-Gal4* and *Cha-Gal4*/*MB-Gal80,* visualized with the *UAS-mCD8::GFP* reporter (grayscale). Arrows indicate that the MB lobes are unlabeled in *Cha-Gal4*/*MB-Gal80*. Scale bar, 50μm. (**B**) Expression patterns (green) of *Cha-Gal4*, *cer-Gal4*, *Ddc-Gal4*, *Trh493-Gal4*, *Trh996-Gal4*, *cry-Gal4*, *per-Gal4*, *CaMKII-Gal4*(X) and *CaMKII-Gal4*(III). Brain samples are counterstained with DLG-antibody immunostaining (magenta). Arrows indicate soma of the two DAL neurons. Scale bar, 50μm.

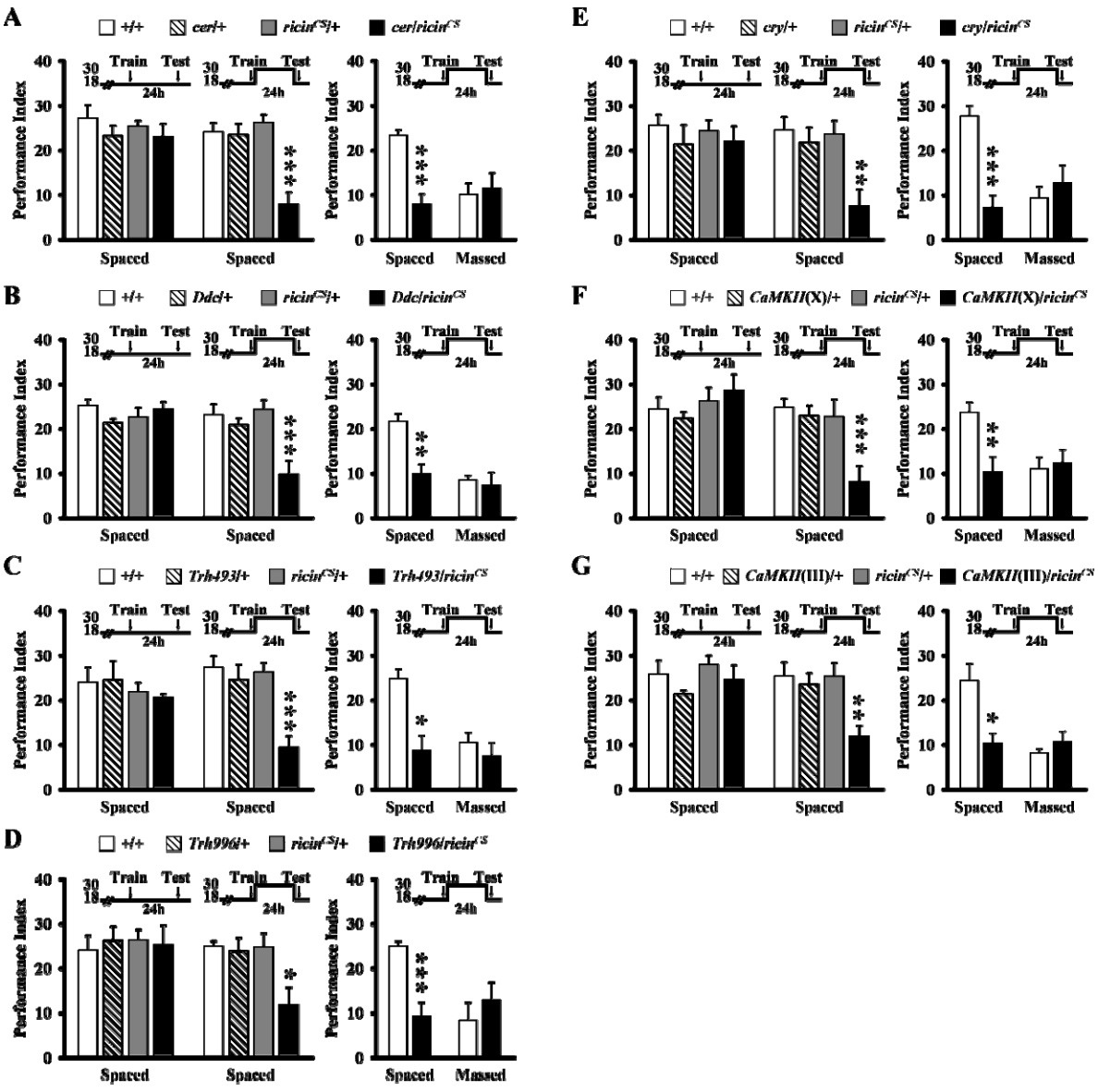

fig. S3. Confirmation of LTM impairments with activated RICIN^{CS} driven by "Cantonized" *Gal4* lines in the experiments balanced with control flies. Inhibition of protein synthesis in *cer-Gal4* **(A)**, *Ddc-Gal4* **(B)**, *Trh493-Gal4* **(C)**, *Trh996-Gal4* **(D)**, *cry-Gal4* **(E)**, *CaMKII-Gal4*(X) **(F)** and *CaMKII-Gal4*(III) **(G)** neurons after training impairs 1-day memory after spaced training but not after massed training. 1-day memory after spaced training is normal when RICIN^{CS} is inactive (in flies kept at 18^{o}C). 1-day memory after spaced, but not massed, training was impaired, when RICIN^{CS} was activated (flies were transferred to 30^{o}C) immediately after training for the entire 24 hours. Values are means $\pm$ S.E.M. (N = 8-12 experiments; * $P< 0.05$; ** $P< 0.01$; *** $P< 0.001$).

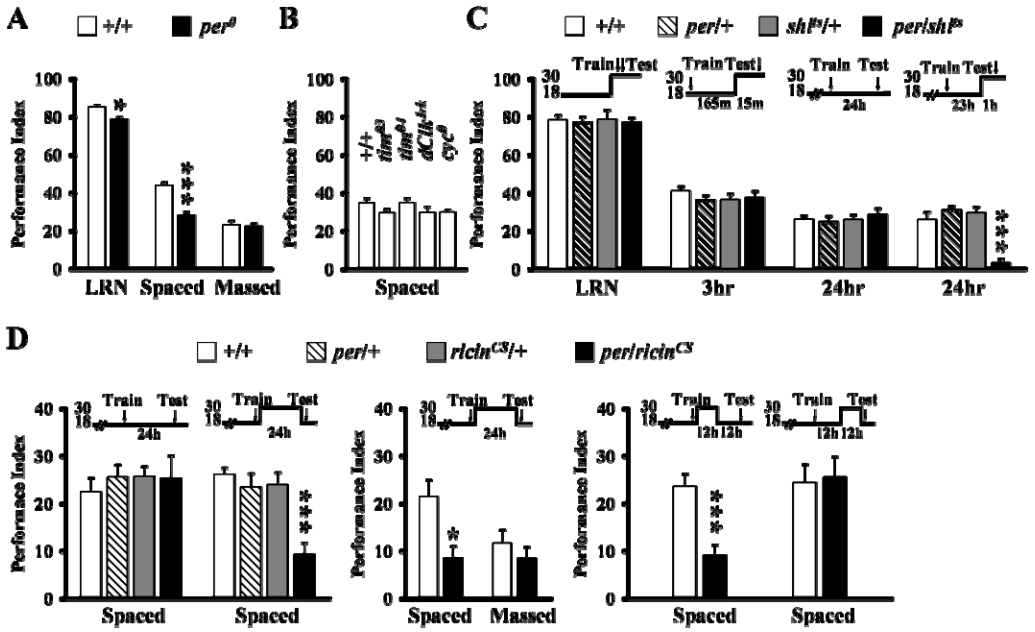

fig. S4. *per-Gal4* neurons are required for LTM formation. (**A**) In the per^0 mutant, memory retention immediately after single training session (LRN) is mildly impaired, and 1-day memory after spaced training is defective and 1-day memory after massed training is not. Values are means ± S.E.M. (N = 8-12 experiments; *, $P< 0.05$; ***, $P< 0.001$). Genotypes: 1) +/+ and 2) per^0/per^0. (**B**) In tim^{03}, tim^{04}, $dClk^{Jrk}$, and cyc^0 mutants, 1-day memory after spaced training is normal. Genotypes: 1) +/+, 2) tim^{03}/tim^{03}, 3) tim^{04}/tim^{04}, 4) $dClk^{jrk}/dClk^{jrk}$ and 5) cyc^0/cyc^0. (**C**) Blocking neurotransmission from *per* neurons during the test trial (retrieval) with *UAS-*shi^{ts} at 30°C impairs 1-day memory retention after spaced training but has no effect on memory immediately or 3-hour after single training session. All flies were raised at 18°C until training began. Control flies kept continuously at 18°C exhibit normal 1-day memory after spaced training. Values are means ± S.E.M. (N = 12 experiments; *, $P< 0.05$; ***, $P< 0.001$). Genotypes: 1) +/+, 2) *per-Gal4*/+, 3) shi^{ts}/+ and 4) *per-Gal4*/+; shi^{ts}/+. (**D**) Inhibition of protein synthesis in *per-Gal4* neurons at different time windows after training impairs 1-day memory after spaced training but not after massed training. 1-day memory after spaced training is normal when $RICIN^{CS}$ is inactive (in flies kept at 18°C). 1-day memory after spaced, but not massed, training was impaired, when $RICIN^{CS}$ was activated (flies were transferred to 30°C) immediately after training for the entire 24 hours. If activated $RICIN^{CS}$ was restricted to the first 12 hours after training, 1-day memory after spaced training again was impaired. If activated $RICIN^{CS}$ was restricted to the last 12 hours after training, however, 1-day memory after spaced training was normal. Values are means ± S.E.M. (N = 8-12 experiments; *, $P <0.05$; ***, $P <0.001$). Genotypes: 1) +/+, 2) *per-Gal4*/+, 3) *UAS-*$ricin^{cs}$/+ and 4) *per-Gal4*/+;*UAS-*$ricin^{cs}$/+.

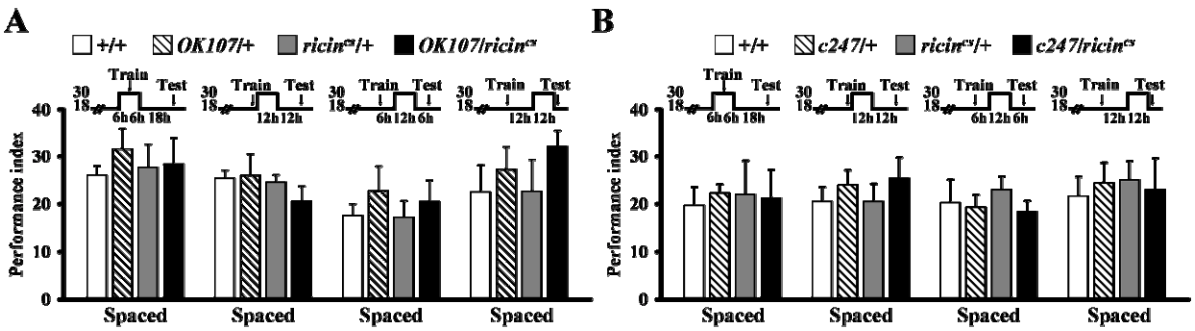

fig. S5. Inhibition of protein synthesis in MB neurons does not impair LTM formation. (**A**) RICIN^{CS} was activated in *OK107-Gal4* neurons during, or for various time-windows after, spaced training. 1-day memory was normal in each case. Values are means ± S.E.M. (N = 8-12 experiments). Genotypes: 1) +/+, 2) *OK107-Gal4*/+, 3) *UAS-ricin^{cs}*/+ and 4) *OK107-Gal4*/+;*UAS-ricin^{cs}*/+. (**B**) RICIN^{CS} was activated in *c247-Gal4* neurons during, or for various time-windows after, spaced training. Again, 1-day memory was normal in each case. Values are means ± S.E.M. (N = 8-12 experiments). Genotypes: 1) +/+, 2) *c247-Gal4*/+, 3) *UAS-ricin^{cs}*/+ and 4) *UAS-ricin^{cs}*/*c247-Gal4*.

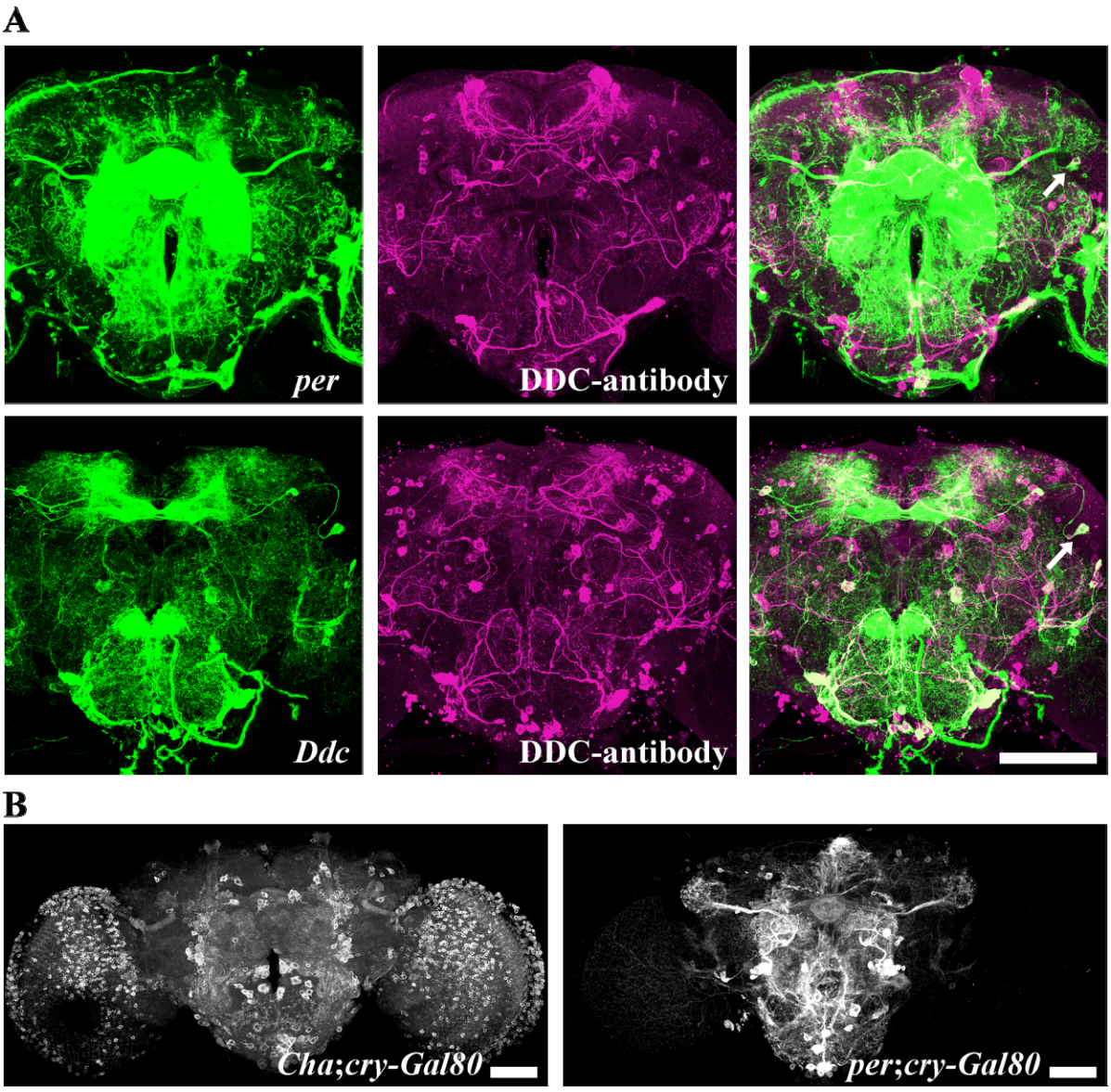

fig. S6. Identification of common neurons in two *Gal4* lines. (**A**) DDC-antibody immunostaining (magenta) of *per-Gal4* and *Ddc-Gal4* neurons, visualized with the *UAS-mCD8::GFP* reporter (green). Arrow indicates a DDC-antibody immunopositive *per* neuron. Scale bar: 50μm. Genotypes: 1) *per-Gal4*/*UAS-mCD8::GFP*;*UAS-mCD8::GFP*/+ and 2) *Ddc-Gal4*/+;*UAS-mCD8::GFP*/+;*UAS-mCD8::GFP*/+. (**B**) Expression patterns of *Cha-Gal4*;*cry-Gal80* and *per-Gal4*;*cry-Gal80*, again visualized with the *UAS-mCD8::GFP* reporter (grayscale). Scale bar, 50μm.

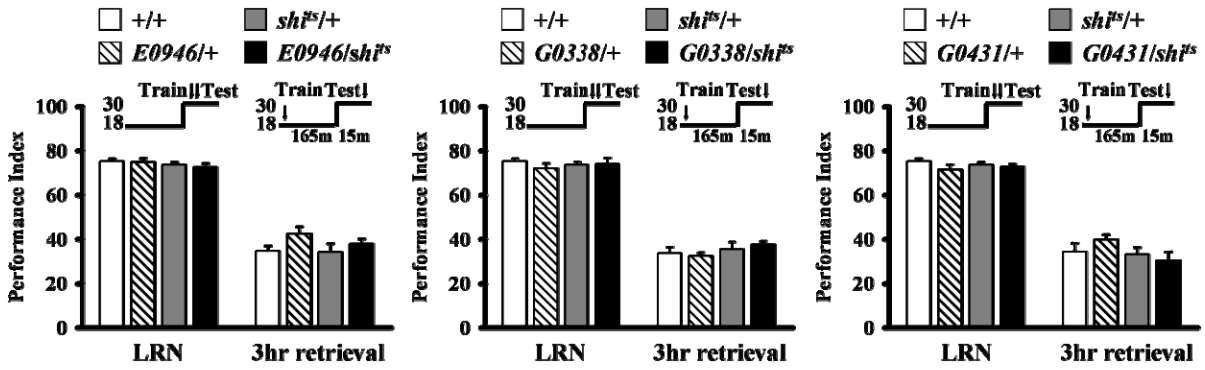

fig. S7. Blocking neurotransmission from DAL neurons does not affect memory retention immediately or 3 hours after single training session. The expression of *UAS-shi^{ts}* is driven by three different DAL-specific *Gal4* lines, *E0946-Gal4*, *G0338-Gal4* and *G0431-Gal4*. Flies were kept at 30^{o}C for the test trial (retrieval). All flies were raised at 18^{o}C until training began. Values are means $\pm$ S.E.M. (N=8 experiments). Genotypes: 1) +/+, 2) *UAS-shi^{ts}*/+, 3) *E0946-Gal4*/+, 4) *E0946-Gal4*/*UAS-shi^{ts}*, 5) *G0338-Gal4*/+, 6) *G0338-Gal4*/+;;*UAS-shi^{ts}*/+, 7) *G0431-Gal4*/+ and 8) *G0431-Gal4*/+;*UAS-shi^{ts}*/+.

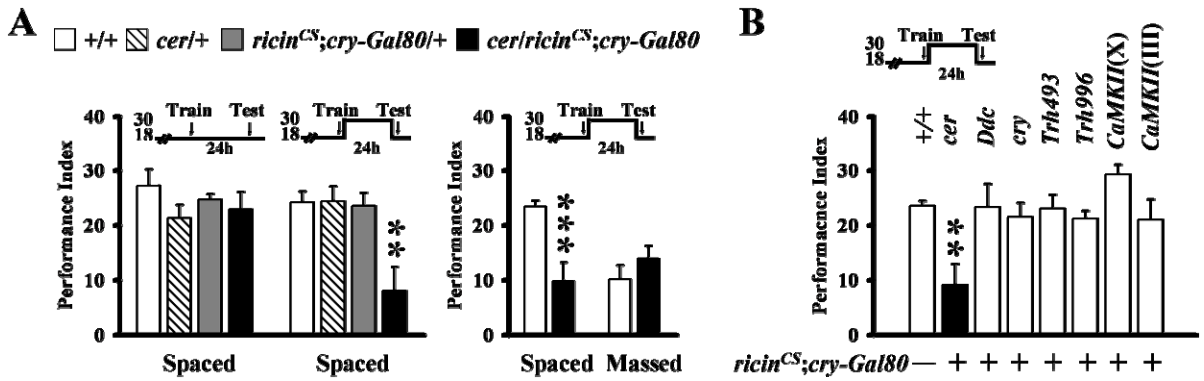

fig. S8. 1-day memory after spaced training is impaired by activated RICIN^{CS} expressed in neurons other than DAL neurons. (**A**) 1-day memory after spaced training was impaired by activated, but not inactivated, RICIN^{CS} in *cer-Gal4* -expressing neurons with DAL neurons "subtracted" by using *cry-Gal80*. Flies were kept at 30^{o}C after training for the entire 24 hours to activate RICIN^{CS}. Genotype: 1) +/+, 2) *cer-Gal4*/+, 3) *UAS-ricin^{cs}*/+;*cry-Gal80*/+ and 4) *cer-Gal4*/*UAS-ricin^{CS}*;*cry-Gal80*/+**.** (**B**) Similar subtractions of DAL neurons using *cry-Gal80* revealed no impairments in 1-day memory after spaced training for *Ddc-Gal4*, *cry-Gal4*, *Trh493-Gal4*, *Trh996-Gal4*, *CaMKII-Gal4*(X) or *CaMKII-Gal4*(III). Values are means $\pm$ S.E.M. (N = 8 experiments; **, $P< 0.01$; ***, $P< 0.001$).

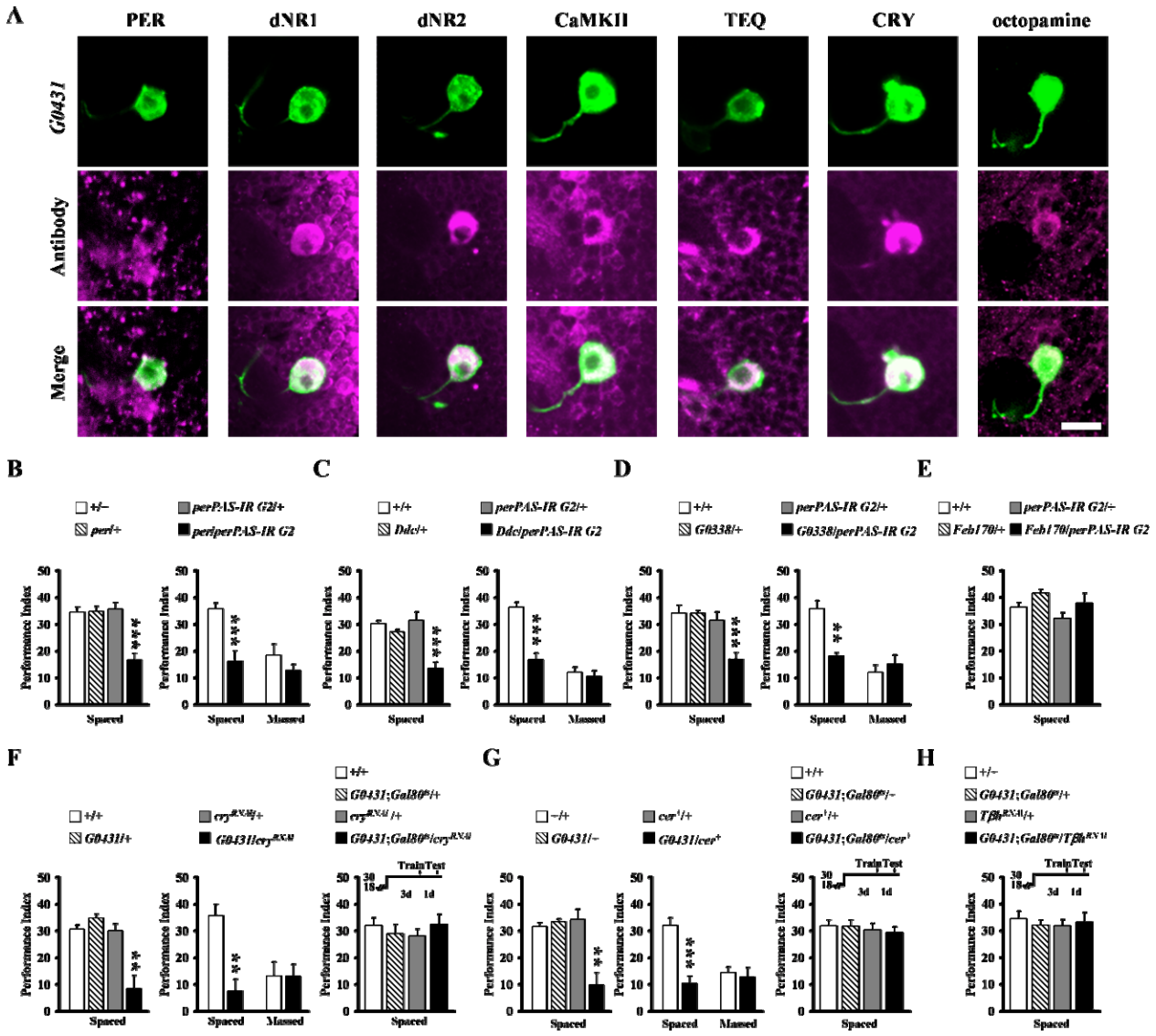

fig. S9. Disruption of genes expressed in DAL neurons impairs 1-day memory after spaced training but not after massed training. (**A**) Immunostaining (magenta) of PER, dNR1, dNR2, CaMKII, TEQUILA, CRY and octopamine in a DAL neuron, visualized with the *UAS-mCD8::GFP* reporter (green). Scale bar, 10μm. (**B-D**) Constitutive disruption of PER in *per-Gal4*, *Ddc-Gal4* or *G0338-Gal4* neurons impairs 1-day memory after spaced, but not massed, training. Genotypes: 1) +/+, 2) *per-Gal4*/+, 3) *UAS-perPAS-IR G2*/+, 4) *per-Gal4*/*UAS-perPAR-IR G2*, 4) *Ddc-Gal4*/+, 5) *Ddc-Gal4*/+;*UAS-perPAR-IR G2*/+, **6**) *G0338-Gal4*/+ and 7) *G0338-Gal4*/+;*UAS-perPAR-IR G2*/+. (**E**) 1-day memory after spaced training remains intact after constitutive disruption of PER in *Feb170-Gal4* neurons. Genotypes: 1) +/+, 2) *Feb170-Gal4*/+, 3) *UAS-perPAS-IR G2*/+ and 4) *Feb170-Gal4*/*UAS-perPAS-IR G2*. **(F)** Constitutive, but not induced, disruption of CRY in DAL neurons impairs 1-day memory after spaced training but not after massed training. Genotypes: 1) +/+, 2) *G0431-Gal4*/+, 3) *UAS-cry*^{RNAi}/+, 4) *G0431-Gal4*/*UAS-cry*^{RNAi}, 5) *G0431-Gal4*/+;*tub-Gal80*^{ts}/+ and

6) *G0431-Gal4*/*UAS-cry*^{RNAi};*tub-Gal80*^{ts}/+. **(G)** Constitutive, but not induced, overexpression of CER in DAL neurons impairs 1-day memory after spaced but not after massed training. Genotypes: 1) +/+, 2) *G0431-Gal4*/+, 3) *UAS-cer*$^{+}$/+, 4) *G0431-Gal4*/*UAS-cer*$^{+}$, 5) *G0431-Gal4*/+;*tub-Gal80*^{ts}/+ and 6) *G0431-Gal4*/*UAS-cer*$^{+}$;*tub-Gal80*^{ts}/+. (**H**) Induced disruption of tyramine β hydroxylase (Tβh) doesn't impair 1-day memory after spaced training. Genotypes: 1) +/+, 2) *G0431-Gal4*/+, 3) *UAS-Tβh*^{RNAi}/+, 4) *G0431-Gal4*/+;*tub-Gal80*^{ts}/+ and 5) *G0431-Gal4*/*UAS-Tβh*^{RNAi};*tub-Gal80*^{ts}/+. For induced expression, flies were raised at 18^{o}C and then transferred to 30^{o}C for 3 days before training to remove *tub-Gal80*^{ts} inhibition and allow *Gal4*-driven expression. In all experiments, values are means $\pm$ S.E.M. (N = 4-12 experiments; **, $P<$ 0.01; ***, $P<$ 0.001).

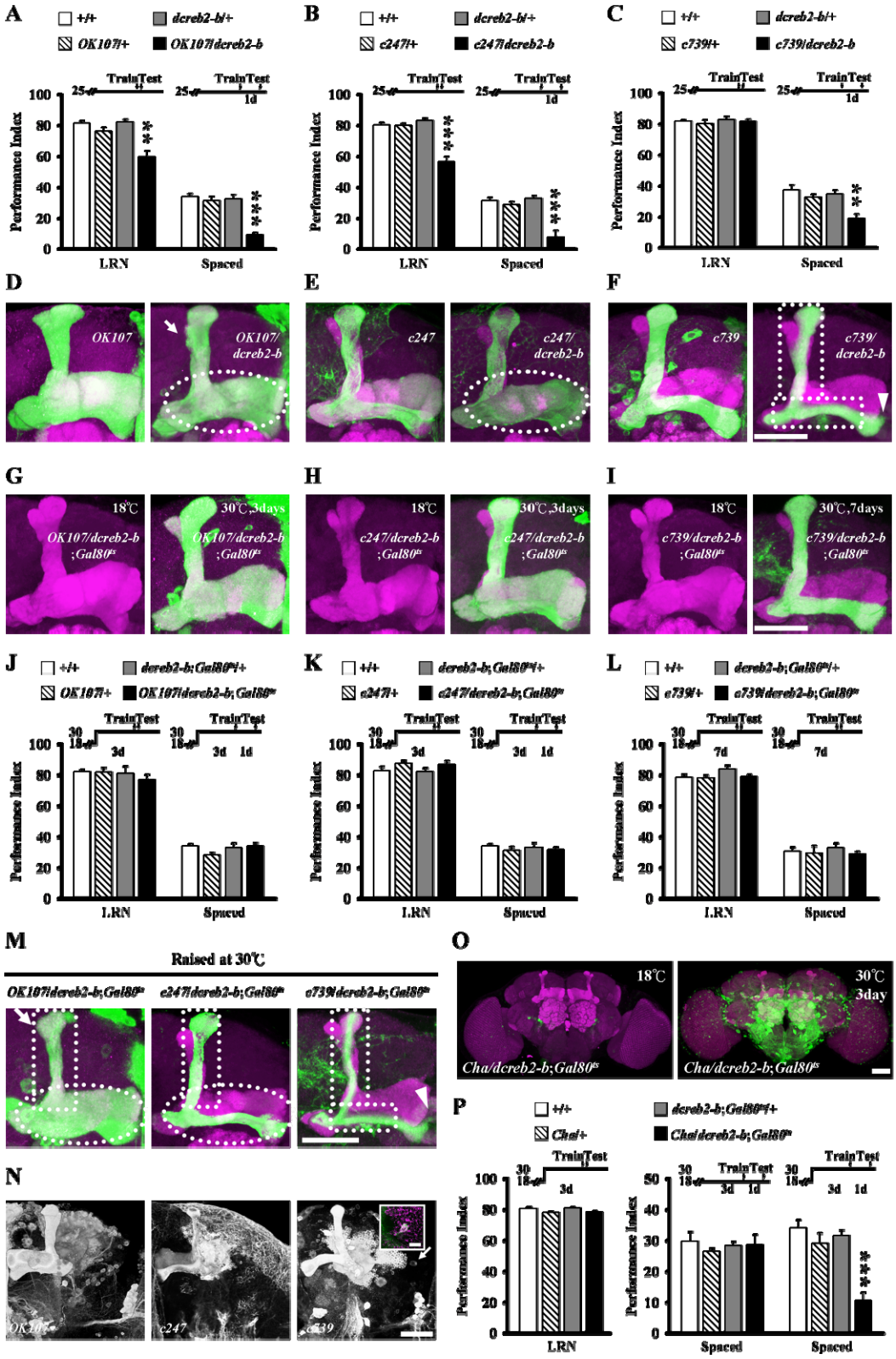

fig. S10. Induced overexpression of CREB2 repressor in MB neurons does not impair 1-day memory after spaced or massed training. (**A-C**) Constitutive expression of CREB2 repressor (*dcreb2b*) in MB

neurons impairs 1-day memory after spaced training. In two *MB-Gal4* lines (*OK107* and *c247*), immediate memory after single training session also is impaired. Genotypes: 1) +/+, 2) *UAS-dcreb2-b*/+, 3) *OK107-Gal4*/+, 4) *UAS-dcreb2-b*/+;;*OK107-Gal4*/+, 5) *c247-Gal4*/+, 6) *UAS-dcreb2-b*/+;;*c247-Gal4*/+, 7) *c739-Gal4*/+ and 8) *UAS-dcreb2-b*/+;*c739-Gal4*/+. (**D-F)** Constitutive expression of CREB2 repressor produces morphological defects in MB neurons. Arrow indicates missing α lobes; dashed circle indicates fewer fibers in γ lobes; arrowhead indicates some αβ axons crossing the midline. Genotypes: 1) *UAS-mCD8::GFP*/+; *UAS-mCD8::GFP*/+;*OK107-Gal4*/+ and 2) *UAS-dcreb2-b*/+;*UAS-mCD8::GFP*/+; *UAS-mCD8::GFP*/+; *OK107-Gal4*/+ (**D**), 1) *UAS-mCD8::GFP*/+; *c247-Gal4*/*UAS-mCD8::GFP* and 2) *UAS-dcreb2-b*/+; *UAS-mCD8::GFP*/+;*c247-Gal4*/*UAS-mCD8::GFP* (**E**), 1) *UAS-mCD8::GFP*/*c739-Gal4*;*UAS-mCD8::GFP*/+ and 2) *UAS-dcreb2-b*/+;*UAS-mCD8::GFP*/*c739-Gal4*; *UAS-mCD8::GFP*/+ (**F**). (**G-I**) Induced expression of CREB2 repressor in MB neurons does not impair immediate memory after single training session or 1-day memory after spaced or massed training. Flies were raised and then at 18°C were transferred to 30°C for at least 3 days before training began, to remove *tub-Gal80^{ts}* inhibition and allow *Gal4*-mediated transgene expression. Genotypes: 1) +/+, 2) *UAS-dcreb2-b*/+; *tub-Gal80^{ts}*/+, 3) *OK107-Gal4*/+, 4) *UAS-dcreb2-b*/+;*tub-Gal80^{ts}*/+;; *OK107-Gal4*/+, 5) *c247-Gal4*/+, 6) *UAS-dcreb2-b*/+;*tub-Gal80^{ts}*/+;*c247-Gal4*/+, 7) *c739-Gal4*/+ and 8) *UAS-dcreb2-b*/+;*tub-Gal80^{ts}*/*c739*. (**J-L**) Induced expression of CREB2 repressor does not produce MB defects. At 18°C, *Gal80* inhibits *Gal4* activity and *UAS-mCD8::GFP* and *UAS-dcreb2-b* are not expressed. MB morphology is revealed with DLG antibody immunostaining (magenta). After three days at 30°C, GFP and *dcreb2-b* are expressed and MB morphology remains intact. Genotypes: *UAS-dcreb2-b*/+;*tub-Gal80^{ts}*/+;*UAS-mCD8::GFP*/+; *OK107-Gal4*/+ (**J**), *UAS-dcreb2-b*/+; *tub-Gal80^{ts}*/+;*c247-Gal4*/*UAS-mCD8::GFP* (**K**), *UAS-dcreb2-b*/+; c739-*Gal4*/*tub-Gal80^{ts}*;*UAS-mCD8::GFP*/+ (**L**). (**M**) When these same flies were raised continuously at 30°C, MB defects were readily apparent as in D-F above. Fiber degeneration was observed in α'β' (arrow), γ (circle), and αβ (square) lobes. In some cases, fibers may across the midline (arrowhead). (**N**) In addition to MB neurons, *c739-Gal4*, but not *OK107-Gal4* or *c247-Gal4,* expressed weakly also in DAL neurons. Scale bar, 50μm. Inset, DAL soma (arrow) weakly labeled by *UAS-mCD8::GFP* was verified by DDC antibody immunostaining (magenta) while fibers are invisible. Scale bar: 10μm. (**O**) Induced expression of *UAS-mCD8::GFP* (green) and *UAS-dcreb2-b* with the *Cha-Gal4* driver after transferring flies to 30°C for three days. GFP expression is not apparent beforehand, when flies are raised at 18°C. Genotypes: *UAS-dcreb2-b*/+; *Cha-Gal4*/*tub-Gal80^{ts}*;*UAS-mCD8::GFP*/+. (**P**) Induced expression of *UAS-dcreb2-b* in *Cha* neurons impaired 1-day memory after spaced training, but not memory retention immediately after single training session (LRN). Flies raised at 18°C were transferred to 30°C to remove *tub-Gal80^{ts}* inhibition of *Gal4* expression for 3 days. Control flies kept at 18°C for 4 days carrying the same transgenes exhibited normal learning and LTM. Genotypes: 1) +/+, 2) *Cha-Gal4*/+, 3) *UAS-dcreb2-b*/+;*tub-Gal80^{ts}*/+ and 4) *UAS-dcreb2-b*/+;*Cha-Gal4*/*tub-Gal80^{ts}*. In all experiments, values are means ± S.E.M. (N = 8-12; ** = $P < 0.01$; *** = $P < 0.001$). Except in (**N**), all brains are counterstained with DLG antibody immunostaining (magenta). Scale bar, 50μm.

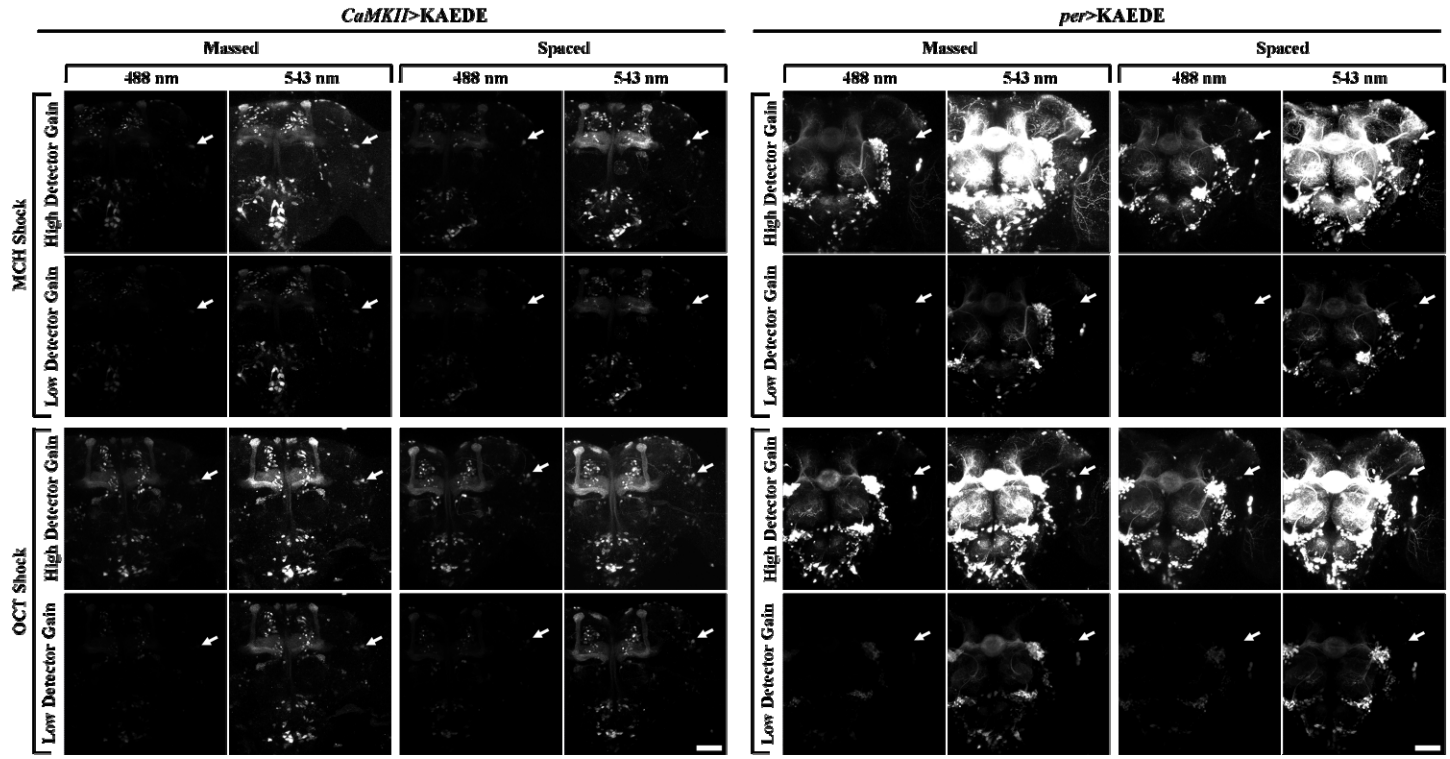

fig. S11. The spaced training-induced elevation of KAEDE synthesis occurred exclusively in the DAL neurons in *per-* and *CaMKII-Gal4*. Living flies were subjected to UV irradiation to convert pre-existing KAEDE into red fluorescence protein just before training. Levels of KAEDE synthesis were quantified 24 hours after spaced or massed training. Whole brain was imaged at two detection sensitivities: high detector gain maximized for the DAL neurons and low detector gain maximized for the MB or the lateral circadian neurons. Except in the DAL neurons, we did not see the spaced training-induced elevation of KAEDE synthesis in any other neurons comparing the 488 channel between massed and spaced training. Arrow: DAL neuron. Scale bar: 50 μm. Genotypes: 1) *CaMKII-Gal4*(III)/*UAS-kaede* and 2) *per-Gal4*/+;*UAS-kaede*/+.

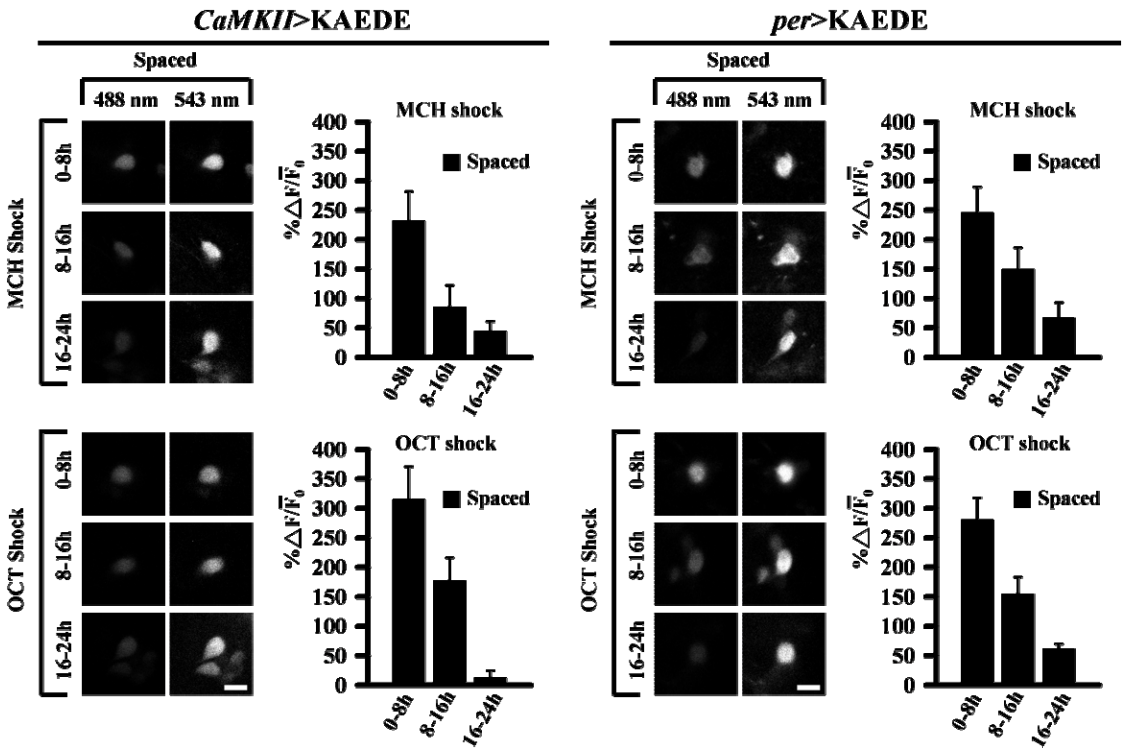

fig. S12. Temporal changes in the elevated *CaMKII* and *per* transcriptional activities in the DAL neurons after spaced training. Living flies were subjected to UV irradiation to convert pre-existing KAEDE into red fluorescence protein just before training, 8 hours after training, or 16 hours after training. Levels of KAEDE were quantified every 8 hours after training. A single optical slice through the cell body of a DAL neuron was taken under the same detection condition for all brains. KAEDE synthesis was determined as the ratio of new (green 488nm) to old (red 543nm) KAEDE in the same neuron (%□F/ $\bar{F}_0$). Scale bar: 10 μm. Values are means± S.E.M. (N=6-16 samples). Genotypes: 1) *CaMKII-Gal4*(III)/*UAS-kaede* and 2) *per-Gal4*/+; *UAS-kaede*/+.

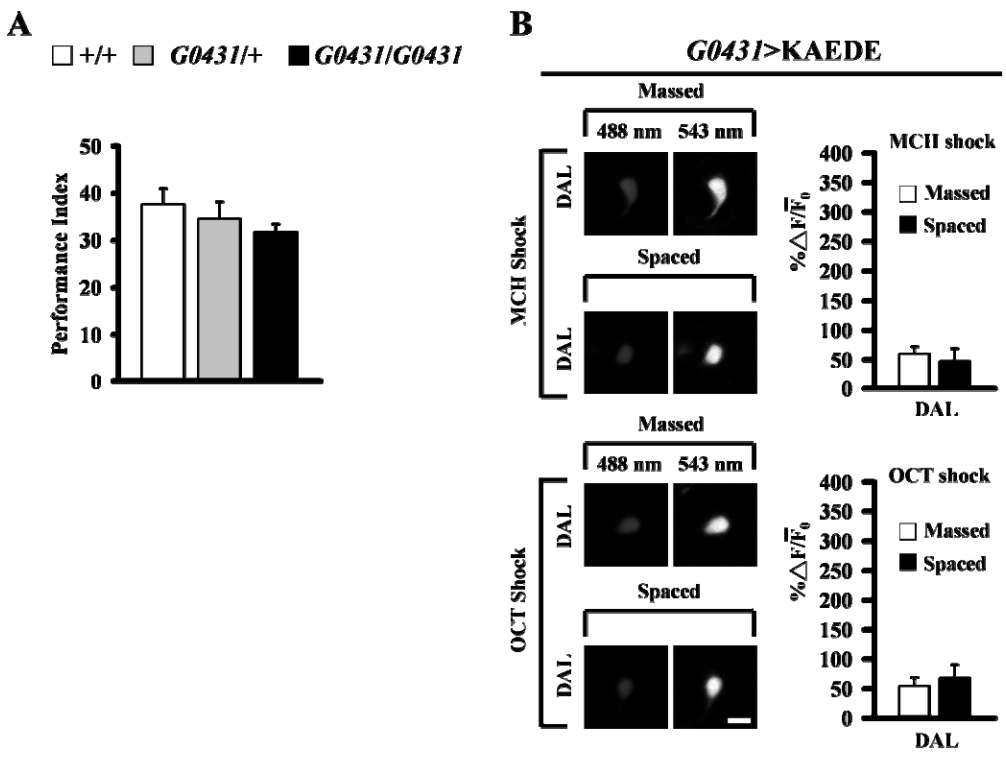

fig. S13. Disruption of an unknown gene expressed in the DAL neurons does not affect 1-day memory after spaced training. (**A**) 1-day memory after spaced training is normal in heterozygous and in homozygous mutants. Values are means± S.E.M. (N=8 experiments). Genotypes: 1) +/+, 2) *G0431*/+ and 3) *G0431*/*G0431*. (**B**) KAEDE synthesis in *G0431-Gal4* flies is not induced by spaced or massed training. Values are means± S.E.M. (N=10-14 samples). Genotype: *G0431*/*UAS-kaede*. Scale bar: 10 μm. Living flies were subjected to UV irradiation to convert pre-existing KAEDE into red fluorescence protein just before training. *UAS-kaede* synthesis was quantified 24 after training. For each brain, a single optical slice through the cell body of a DAL neuron was taken under the same detection conditions. KAEDE synthesis was determined as the ratio of new (green 488nm) to old (red 543nm) KAEDE within each fly brain ($\%\triangle F/\ \bar{F}_0$).

Gal4 drivers	APL	DAL	DPM	EB	glia	MB	eye	OSN	PN
c42	-	-	-	+++	-	-	-	-	-
c217	-	-	-	+++	-	-	-	-	+
c247	-	-	-	-	+	+++	-	-	-
c305a	-	-	-	++	+	++	+	-	-
c316	-	N.D.	+++	-	+++	++	++	-	-
c507	-	-	-	+++	-	-	-	-	-
c739	-	+	-	+	-	+++	+	-	-
c772	-	N.D.	-	+	-	+++	-	-	-
CaMKII (X)	-	+++	-	-	-	+++	+	-	-
CaMKII (III)	-	+++	-	-	-	+++	+	-	-
cer	-	++	-	-	-	+++	+	-	-
Cha	N.D.	++	N.D.	+++	-	+++	+++	N.D.	+
cry	-	+	-	++	++	+++	-	-	-
Ddc	-	++	-	-	-	-	+	-	-
dTdcII	-	-	-	-	-	-	-	-	-
DVGLUT	-	-	-	+++	-	+	++	N.D.	+
E0973	-	-	-	++	-	+++	-	-	-
Feb170	-	-	-	+++	-	-	++	-	-
G0050	-	N.D.	-	+	+	+++	+	-	-
Gad	N.D.	-	+	+++	-	+++	++	-	++
GH146	++	-	-	-	-	-	+	-	+++
GMR	-	-	-	-	-	-	+++	-	-
OK107	-	-	-	+	-	+++	+	-	-
Or83b	-	-	-	-	-	-	-	+++	-
P0010	-	-	-	+++	++	-	-	-	-
per	-	+	-	+++	+	-	+	-	++
repo	-	-	-	-	++	-	-	-	-
TH	-	-	-	++	-	-	+	-	-
tim14-27	-	-	-	-	+++	-	++	N.D.	+
tim14-82	-	-	-	-	+++	-	++	N.D.	+
Trh493	-	++	+++	-	-	-	+	N.D.	N.D.
Trh996	-	+	-	+++	-	-	++	-	-

Table S1. Gal4 expression patterns. The GFP intensity reported by *Gal4>UAS-mCD8::GFP;UAS-mCD8::GFP* was graded as strong (+++), intermediate (++), weak (+), absence (-) or non-distinguishable (N.D.). APL, anterior paired lateral neurons; DAL, dorsal anterior lateral neuron; DPM, dorsal paired medial neuron; EB, ellipsoid body; MB, mushroom body; OSN, olfactory sensory neuron; PN, projection neuron.

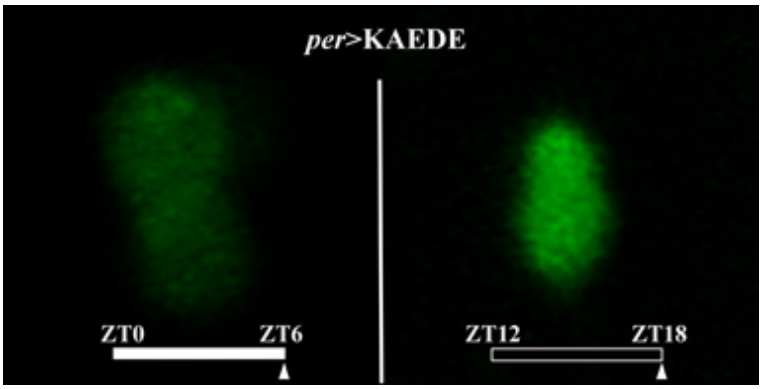

Movie S1. Visualizing *de novo* KAEDE synthesis in *per* neurons during ZT0-6 and ZT12-18, respectively. Circadian transcriptional activity of *per* in the lateral neurons reported by *de novo* synthesis of KAEDE driven by *per-Gal4*. To reset pre-existing green KAEDE, the brain incubated in DDM2 culture medium was UV irradiated for 20s at ZT0 or ZT12. Changes in KAEDE levels were monitored every 20 minutes with a single optical section through cell bodies of lateral neurons during ZT0-6 (left movie) or ZT12-18 (right movie). Genotype: *per-Gal4*/+; *UAS-kaede*/+. driven

Materials and Methods

Fly strains. Fly stocks were maintained on standard corn meal/yeast/agar medium at 25 ± 1°C or 18 ± 1°C and 70% relative humidity on a 12h:12h light:dark cycle. The fly lines used were wild-type Canton-S w1118 (iso1CJ), *UAS-kaede*, *UAS-ricin*^{CS} (from C. J. O'Kan), *UAS-shi*^{ts}, *UAS-perPAS-IR G2* (from M. W. Young), *UAS-CaMKII*^{hpn} (from S. Kunes), *UAS-dcreb2-b* (from L. Davis); *Ddc-Gal4*, *Trh493-Gal4* and *Trh996-Gal4* (from J. Hirsh); *per-Gal4* and *tim-Gal4* (from J. Hall), *cry-Gal4* (from J. Blau); *cry-Gal80* (from M. Rosbash); *MB-Gal80* (from S. Waddell); *CaMKII-Gal4*(X) and *CaMKII-Gal4*(III) (from Y. Takamatsu); *cer-Gal4*, *repo-Gal4*, *UAS-teq41* and *UAS-cer*$^{+}$ (from T. Préat); *lexAop-rCD2::GFP* and *UAS-Dscam::GFP* (from T. Lee); *UAS-CD4::GFP*$_{1\text{-}10}$ and *lexAop-CD4::GFP*$_{11}$ (from K. Scott); *c42*, *c217*, *c247*, *c305a*, *c316*, *c507*, *c739* and *c772* (from S. Benzer); *UAS-cry*^{RNAi} (v105172), *UAS-creb2*^{RNAi} (v101512), *UAS-Ddc*^{RNAi} (v3330), *UAS-Trh*^{RNAi} (v35240) and *UAS-Tβh*^{RNAi} (v51667) (from VDRC). All other flies including *E0946 (112097), E0973 (112178), G0338 (12740)*, *G0431 (12837)* and *P0010 (2023)* were derived from DGRC or Bloomington stock centers.

Behavior. Olfactory associative learning was evaluated by training 2- to 3-day-old flies in a T-maze apparatus with a Pavlovian olfactory conditioning procedure (*44*). Odors used were 3-octanol (OCT) and 4-methylcyclohexanol (MCH). Each experiment consisted of two groups of approximately 100 flies, each of which was conditioned with one of these two odors. Flies were exposed sequentially to two odors which were carried through the training chamber in a current of air (odors were bubbled at 750 ml/min). Flies first were exposed for 60 s to the conditioned stimulus (CS^{+}), during which time they received the unconditioned stimulus (US), which consisted of twelve 1.5 s pulses of 60V DC electric shock at 5 s interpulse intervals. After the presentation of CS^{+}, the chamber was flushed with fresh air for 45 s. Then, flies were exposed for 60 s to the CS^{-}, which was not paired with the US. This procedure constitutes single training session. For 24-hour memory experiments, flies were subjected to ten such training sessions, either massed together without rest or spaced out with a 15 min rest interval. For these multiple training protocols, robotic trainers were used. The test was carried out in the dark in an environment-controlled room at required temperatures and 70% relative humidity. Except in the initial behavioral screen (Fig. 2 and fig. S8B), genetic backgrounds of all fly strains were equilibrated to the "Canton" wild-type background by five or more generations of backcrossing. All genotypes were trained and tested in parallel and rotated between all of the robotic trainers to ensure a balanced experiment. In RICIN^{CS} experiments, flies raised at 18^{o}C were transferred to 30^{o}C for 24 hours to allow enough RICIN^{CS} expression and then kept under 18^{o}C for another 24 hrs to inactivate RICIN^{CS} before experiments. In *tub-Gal80*^{ts} experiments, flies raised at 18^{o}C were transferred to 30^{o}C for at least 3 days before experiments. For blocking protein synthesis, flies were fed with 35mM cycloheximide 1 day before

training until just before the test (*1*).

To evaluate memory retention immediately after single training session (acquisition), flies were gently tapped into an elevator-like compartment immediately after training. After 90 s, the flies were transported to the choice point of a T maze, in which they were exposed to two converging currents of air (one carrying OCT, the other MCH) from opposite arms of T maze. Flies were allowed to choose between the CS^+ and CS^- for 120 s, at which time they were trapped inside their respective arms of the T maze (by sliding the elevator out of register), anesthetized and counted. Flies that chose to avoid the CS^+ ran into the T maze arm containing the CS^-,while flies that chose to avoid the CS^- ran into the T maze arm containing the CS^+. To assay 3 hr memory retention after single training session, trained flies were placed in a food tube in the dark until tested in the T maze apparatus. For each experiment, performance index $PI_{1,2} = (N_{\text{non punished}} - N_{\text{punished}})/(N_{\text{non punished}} + N_{\text{punished}})$ was calculated and averaged over these two complimentary experiments, with the final $PI = (PI_1+PI_2)/2$. Averaging of the two reciprocal scores eliminates possible bias originating from machine, naïve odor preferences or nonassociative changes in olfaction.

KAEDE measurement. To measure the amount of newly synthesized KAEDE in single neurons, we used the following procedures. (i) Pre-existing KAEDE proteins were photoconverted into red fluorescence proteins by 365-395 nm UV irradiation generated from a 120W mercury lamp. Two methods were used (fig. S1). To monitor circadian synthesis in *per* neurons, a single fly restricted in a pipette tip was UV irradiated for 5 min through an objective lens (N.A. value 0.5, working distance 2mm). For the behavior assay, approximately 100 flies kept in a clear plastic syringe were directly exposed to UV light at a distance of 5cm for 1 hour. (ii) Individual single neurons expressing KAEDE were directly visualized through an open window of the fly's head capsule. Living samples were used because the signal to noise ratio of green versus red KAEDE is greatly reduced after chemical fixation. (iii) KAEDE neurons were located in less than 5 seconds by a fast pre-scanning of red KAEDE excited by a 543nm laser to avoid unnecessary fluorescence quenching of green KAEDE during repeated scanning. (iv) A single optical slice through cell bodies at a resolution of 1024x1024 pixels was imaged under a confocal microscope with a 40X C-Apochromat water-immersion objective lens (N.A. value 1.2, working distance 220μm). All brain samples in the experiment were imaged with the same optical setting maximized for green and red KAEDE immediately before and after photoconversion, respectively. (v) In all cases, both green KAEDE excited by a 488 nm laser and red KAEDE excited by 543 nm laser were measured. We found that red KAEDE is very stable with less than 2% decay rate in 24 hours. Using the amount of red KAEDE as an internal standard to calibrate individual variation, we calculated the increasing rate of green KAEDE synthesis after photoconversion with the formula $(\Delta F)=\%(F_{t1}- \overline{F}_{t0})/ \overline{F}_{t0}$, where

F_{t1} and F_{t0} are the ratio of averaged intensities between green (G) and red (R) KAEDE (G_{t0}/R_{t0}) immediately after photoconversion ($_{t0}$) and at a specific later time point ($_{t1}$), respectively.

Immunohistochemistry. Brains were dissected in phosphate-buffered saline (PBS), heated with a commercial microwave oven in 4% paraformaldehyde on ice for 60 seconds three times, and then in 4% paraformaldehyde with 0.25% Triton X-100 for 60 seconds three times. After being washed in PBS for 10 min at room temperature, brain samples were incubated in PBS containing 2% Triton X-100 and 10% normal goat serum and degassed in a vacuum chamber to expel tracheal air for four cycles (depressurize to -70 mmHg then hold for 10 minutes). Next, brain samples were blocked and penetrated in PBS-T at 4°C overnight and then incubated in PBS-T containing one of the following primary antibodies: (1) 1:500 rat anti-DDC polyclonal antibody (from J. Hirsh), (2) 1:40 mouse 4F3 anti-DLG antibody (Developmental Studies Hybridoma Bank, Univ. of Iowa), (3) 1:5000 rabbit anti-CaMKII polyclonal antibody (from L. C. Griffith), (4) 1:300 guinea pig anti-CRY (from P. E. Hardin), (4) 1:1000 rabbit anti-dNR1 polyclonal antibody (α-85S), (5) 1:500 rabbit anti-dNR2 polyclonal antibody (α-820-1, α-820-2), (6) 1:500 rabbit anti-TEQUILA polyclonal antibody (from T. Préat), (7) 1:10000 rabbit anti-PER polyclonal antibody (from Jeffrey L. Price) and (8) 1:500 rabbit anti-octopamine (from Millipore. AB1799) at 4°C for 1 day. After being washed in PBS-T three times, samples were incubated in PBS-T containing one of the following secondary antibodies: (1) 1:200 biotinylated goat anti-mouse IgG (Molecular Probes), (2) 1:200 biotinylated goat anti-rat IgG, (3) 1:200 biotinylated goat anti-rabbit IgG, and (4) 1:200 biotinylated goat anti-guinea pig IgG at 25°C for 1 day. Next, brain samples were washed and incubated with 1:500 Alexa Fluor 635 streptavidin (Molecular Probes) at 25°C for 1 day. Finally, after extensive washing, immunolabeled brain samples were directly cleared in *FocusClear*, an aqueous solution that renders biological tissue transparent (*45*), for 5 min and mounted between two cover slips separated by a spacer ring of ~200μm in thickness. Sample brains were imaged under a Zeiss LSM 710 confocal microscope with a 40X C-Apochromat water-immersion objective lens (N.A. value 1.2, working distance 220μm).

Statistics. All the raw data were analyzed parametrically with JMP5.1 statistical software. As a result of the nature of their mathematical derivation, performance indexes were distributed normally. Hence, the data were evaluated via one-way ANOVAs. Subsequent pair-wise planned comparisons were adjusted for experiment-wise error (α′), keeping the overall $\alpha = 0.05$. All data were presented as means$\pm$ S.E.M.

References

1. T. Tully, T. Préat, S. C. Boynton, M. Del Vecchio, *Cell* **79**, 35 (1994).

2. J. C. Yin *et al*., *Cell* **79**, 49 (1994).

3. R. L. Davis, *Neuron* **70**, 8 (2011).

4. D. Yu, D. B. Akalal, R. L. Davis, *Neuron* **52**, 845 (2006).

5. M. Heisenberg, *Nat. Rev. Neurosci.* **4**, 266 (2003).

6. B. Gerber, H. Tanimoto, M. Heisenberg, *Curr. Opin. Neurobiol.* **14**, 737 (2004).

7. D. B. Akalal, D. Yu, R. L. Davis, *J. Neurosci.* **30**, 16699 (2010).

8. D. B. Akalal, D. Yu, R. L. Davis, *J. Neurosci.* **31**, 5643 (2011).

9. R. Ando, H. Hama, M. Yamamoto-Hino, H. Mizuno, A. Miyawaki, *Proc. Natl. Acad. Sci. U.S.A.* **99**, 12651 (2002).

10. H. Mizuno *et al*., *Mol. Cell* **12**, 1051 (2003).

11. P. E. Hardin, J. C. Hall, M. Rosbash, *Nature* **343**, 536 (1990).

12. Y. Endo, K. Mitsui, M. Motizuki, K. Tsurugi, *J. Biol. Chem.* **262**, 5908 (1987).

13. Y. Endo, K. Tsurugi, *J. Biol. Chem.* **262**, 8128 (1987).

14. K. G. Moffat, J. H. Gould, H. K. Smith, C. J. O'Kane, *Development* **114**, 681 (1992).

15. A. S. Chiang *et al*., *Curr. Biol.* **21**, 1 (2011).

16. T. Riemensperger, T. Völler, P. Stock, E. Buchner, A. Fiala, *Curr. Biol.* **15**, 1953 (2005).

17. A. Claridge-Chang *et al*., *Cell* **139**, 405 (2009).

18. Y. Aso *et al*., *Curr. Biol.* **20**, 1445 (2010).

19. S. I. Ashraf, A. L. McLoon, S. M. Sclarsic, S. Kunes, *Cell* **124**, 191 (2006).

20. A. Pascual, T. Préat, *Science* **294**, 1115 (2001).

21. C. L. Wu *et al*., *Nat. Neurosci.* **10**, 1578 (2007).

22. M. P. Belvin, H. Zhou, J. C. Yin, *Neuron* **22**, 777 (1999).

23. T. Sakai, T. Tamura, T. Kitamoto, Y. Kidokoro, *Proc. Natl. Acad. Sci. U.S.A.* **101**, 16058 (2004).

24. J. Dubnau, L. Grady, T. Kitamoto, T. Tully, *Nature* **411**, 476 (2001).

25. S. E. McGuire, P. T. Le, R. L. Davis, *Science* **293**, 1330 (2001).

26. S. Xia *et al*., *Curr. Biol.* **15**, 603 (2005).

27. H. H. Lin, J. S. Lai, A. L. Chin, Y. C. Chen, A. S. Chiang, *Cell* **128**, 1205 (2007).

28. M. D. Gordon, K. Scott, *Neuron* **61**, 373 (2009).

29. S. Martinek, M. W. Young, *Genetics* **156**, 1717 (2000).

30. S. E. McGuire, P. T. Le, A. J. Osborn, K. Matsumoto, R. L. Davis, *Science* **302**, 1765 (2003).

31. G. Didelot *et al*., *Science* **313**, 851 (2006).

32. F. V. Bolduc, K. Bell, H. Cox, K. S. Broadie, T. Tully, *Nat. Neurosci.* **11**, 1143 (2008).

33. G. Isabel, A. Pascual, T. Préat, *Science* **304**, 1024 (2004).

34. J. Séjourné *et al*., *Nat. Neurosci.* **14**, 903 (2011).

35. D. Comas, F. Petit, T. Préat, *Nature* **430**, 460 (2004).

36. A. Pascual, K. L. Huang, J. Neveu, T. Préat,. *Nature* **427**, 605 (2004).

37. J. Dubnau *et al*., *Curr. Biol.* **13**, 286 (2003).

38. R. Bourtchuladze *et al*.,. *Cell* **79**, 59 (1994).

39. A. C. Keene, S. Waddell, *Nat. Rev. Neurosci.* **8**, 341 (2007).

40. X. Liu, R. L. Davis, *Nat. Neurosci.* **12**, 53 (2009).

41. C. L. Wu *et al*., *Curr. Biol.* **21**, 848 (2011).

42. J. L. Pitman *et al*., *Curr. Biol.* **21**, 855 (2011).

43. K. G. Moffat, J. H. Gould, H. K. Smith, C. J. O'Kane, *Development* **114**, 681 (1992).

44. T. Tully, W. G. Quinn, *J. Comp. Physiol. A Neuroethol. Sens. Neural Behav. Physiol.* **157**, 263 (1985).

45. A. S. Chiang *et al*., *J. Comp. Neurol.* **440**, 1 (2001).

Ode to the Mushroom Bodies

Josh Dubnau

Science **335**, 664 (2012);
DOI: 10.1126/science.1218171

NEUROSCIENCE

Ode to the Mushroom Bodies

Neurons that stabilize memory storage are located outside of a region in the insect brain long thought to handle this task.

Josh Dubnau

Immediately after a behavioral experience, our memories are rich and vibrant but fragile. Over time, memory of an event or experience begins to fade, but we typically remember the important details because memories become consolidated into a form that is resistant to the passage of time and disruption. Invertebrate animal models, including the fruit fly *Drosophila melanogaster,* have been used to elucidate mechanisms of consolidation that rely on biochemical signaling within a neuron (*1*, *2*). By contrast, most investigations of communication between brain regions for systems-level consolidation have focused on vertebrate animals, based on the assumption that larger, more complex brains are capable of more elaborate processing of memory over time (*3*, *4*). However, several recent studies have provoked a systems view of fruit fly memory (*5*–*7*), and on page 678 of this issue, Chen *et al*. (*8*) provide an even stronger push in that direction.

Conversion of short-term memory (STM) to long-term memory (LTM) involves gene expression under control of the transcription factor cyclic adenosine monophosphate (cAMP)–response element binding protein (CREB) (*9*, *10*). In the *Drosophila* olfactory model, memory formation involves cAMP signaling within neurons of a brain region called mushroom bodies (MBs) (*1*, *2*). The surprising finding of Chen *et al*. is that CREB-dependent gene transcription and protein synthesis required for LTM does not occur in MBs, where olfactory learning takes place, but in a pair of neurons called DAL (see the figure). This result, and the additional role of ellipsoid body neurons (*6*), forces us to think of memory consolidation in the fly in the context of a larger brain system.

The perception of an odor in *Drosophila* is represented as a pattern of neural activity within the MB. If the odor is presented along with a strong reinforcement in the form of reward or punishment, the MBs receive neuromodulatory inputs (such as dopamine in response to an electric shock). The simultaneous stimuli (odor and dopamine) trigger a cellular mechanism called "coincidence detection." For example, stimulation of dopamine receptors in a MB neuron that also experiences an increase in intracellular calcium concentration driven by the odor leads to synergistic activation of an adenylyl cyclase (called *rutabaga*), leading to synthesis of cAMP. This boost in cAMP concentration results in local modifications of synaptic strength. Such coincidence detection likely occurs in the subset of MB neurons that respond to a particular odor and underlies changes in the responses of those neurons the next time the odor is presented.

How does consolidation take place in this model? It involves cAMP-dependent signaling to CREB, which orchestrates gene expression to stabilize the learning-driven modifications to the cell's synapses. This biochemical consolidation mechanism is thought to maintain changes that took place earlier within the same neurons when the coincidence detection occurred in MB neurons. This is why the requirement of CREB-mediated gene expression in DAL neurons and not in MB neurons for LTM is such a conceptual jolt.

Chen *et al*. pinpointed the site of new protein synthesis during memory consolidation in *Drosophila* through cell-specific genetic manipulation in the fly brain. The authors assessed the effect of blocking protein synthesis [by expressing a temperature-sensitive version of a toxin ($RICIN^{CS}$) to inhibit ribosomes] in different subsets of neurons or neuron cell types. This led to the identification of DAL neurons as a necessary location for protein synthesis during memory consolidation. More surprisingly, however, protein synthesis appears to be dispensable in MBs. This observation was validated using a photoconvertible fluorescent protein (KAEDA) to detect de novo protein synthesis. The gene encoding KAEDA was expressed in the subsets of neurons in the fly brain using regulatory regions of genes that are normally activated

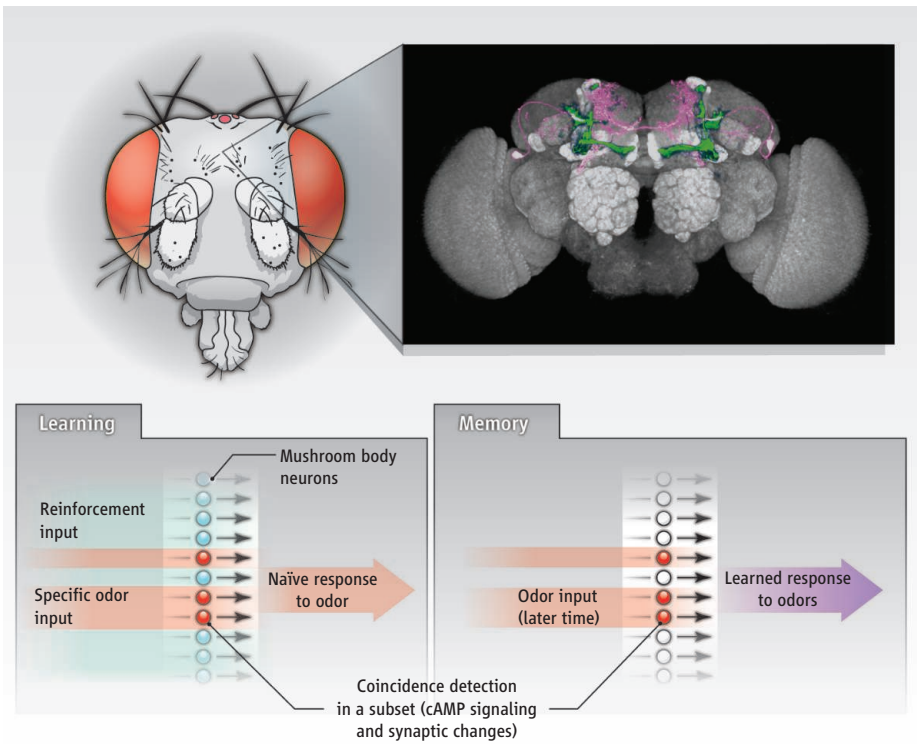

Memory consolidation. (**Top**) The synthesis of new proteins underlying olfactory memory storage takes place in a different anatomical location (DAL neurons, pink) than the brain region where memory is stored [mushroom bodies (MBs)]. DAL neurons appear to form synapses with a subset of MB pioneer α/β neurons (green). (**Bottom**) Odor inputs during learning are represented as a pattern of neural activity within a sparse subset (red) of MB neurons. Punishment drives neuromodulatory inputs (such as dopamine) to all MB neurons (blue). Coincidence detection occurs within neurons that receive both signals. This drives cAMP-dependent synaptic changes that alter the response of the network when the odor is encountered later.

CREDIT (TOP LEFT AND BOTTOM PANELS): Y. HAMMOND/*SCIENCE*; PHOTO (TOP RIGHT PANEL): C.-C. CHEN AND A. S. CHIANG

Cold Spring Harbor Laboratory, Cold Spring Harbor, NY 11724, USA. E-mail: dubnau@cshl.edu

Published by AAAS

during memory formation. This revealed an acute induction of KAEDA expression in DAL neurons but not in MBs during memory consolidation. Thus, protein synthesis occurs and is required in DAL neurons but is neither required nor detected in MBs. It is possible that low levels of protein synthesis in MBs escape the RICIN^{CS} effect and are below detection with KAEDA. However, Chen *et al*. further investigated this question by genetic manipulations of CREB function. They demonstrated that CREB-mediated gene transcription is required for LTM in DAL neurons but not MBs as previously thought (*11*, *12*).

The role for CREB-dependent gene expression in DAL neurons but not MBs is at first hard to understand for two reasons. Expression of the adenylyl cyclase *rutabaga* in MBs is sufficient to support both STM (*13*, *14*) and LTM (*5*, *15*). Thus, CREB function in DAL neurons is not downstream in a signaling sense from *rutabaga* action in MB. There is much evidence that olfactory stimuli are represented as a pattern of activity within MBs and that the associative memory forms there. In principle, olfactory memory could be initiated in one place and then transferred to another during consolidation. But it seems implausible that a few DAL neurons can represent the olfactory percept and also "store" LTM. Instead, a view emerges in which the consolidated memory is distributed within a neural circuit that includes MBs, DAL neurons, and ellipsoid neurons (*6*). Indeed, Chen *et al*. report that DAL axons likely are presynaptic to a subset of MB neurons called pioneer α/β neurons. Although this suggests that MBs are postsynaptic to DAL neurons, the role of gene transcription and protein synthesis within DAL neurons that is driven by coincidence detection in MB neurons also suggests that MBs are upstream of DAL neurons (presynaptic). Taken together, the simplest interpretation is a MB-DAL-MB feedback loop, perhaps including ellipsoid body neurons (*6*). The next task will be to integrate the established biochemical and emerging systems views of consolidation.

References

1. A. C. Keene, S. Waddell, *Nat. Rev. Neurosci.* **8**, 341 (2007).
2. S. E. McGuire, M. Deshazer, R. L. Davis, *Prog. Neurobiol.* **76**, 328 (2005).
3. S. H. Wang, R. G. Morris, *Annu. Rev. Psychol.* **61**, 49, (C1) (2010).
4. P. K. Dash, A. E. Hebert, J. D. Runyan, *Brain Res. Brain Res. Rev.* **45**, 30 (2004).
5. A. L. Blum, W. Li, M. Cressy, J. Dubnau, *Curr. Biol.* **19**, 1341 (2009).
6. C. L. Wu *et al*., *Nat. Neurosci.* **10**, 1578 (2007).
7. M. J. Krashes, A. C. Keene, B. Leung, J. D. Armstrong, S. Waddell, *Neuron* **53**, 103 (2007).
8. C.-C. Chen *et al*., *Science* **335**, 678 (2012).
9. J. C. Yin, T. Tully, *Curr. Opin. Neurobiol.* **6**, 264 (1996).
10. A. J. Silva, J. H. Kogan, P. W. Frankland, S. Kida, *Annu. Rev. Neurosci.* **21**, 127 (1998).
11. D. Yu, D. B. Akalal, R. L. Davis, *Neuron* **52**, 845 (2006).
12. D. B. Akalal *et al*., *J. Neurosci.* **30**, 16699 (2010).
13. T. Zars, M. Fischer, R. Schulz, M. Heisenberg, *Science* **288**, 672 (2000).
14. S. E. McGuire, P. T. Le, A. J. Osborn, K. Matsumoto, R. L. Davis, *Science* **302**, 1765 (2003).
15. S. Trannoy, C. Redt-Clouet, J. M. Dura, T. Preat, *Curr. Biol.* **21**, 1647 (2011).

10.1126/science.1218171

MATHEMATICS

Critical Truths About Power Laws

Most reported power laws lack statistical support and mechanistic backing.

Michael P. H. Stumpf[1] and Mason A. Porter[2]

The ability to summarize observations using explanatory and predictive theories is the greatest strength of modern science. A theoretical framework is perceived as particularly successful if it can explain very disparate facts. The observation that some apparently complex phenomena can exhibit startling similarities to dynamics generated with simple mathematical models (*1*) has led to empirical searches for fundamental laws by inspecting data for qualitative agreement with the behavior of such models. A striking feature that has attracted considerable attention is the apparent ubiquity of power-law relationships in empirical data. However, although power laws have been reported in areas ranging from finance and molecular biology to geophysics and the Internet, the data are typically insufficient and the mechanistic insights are almost always too limited for the identification of power-law behavior to be scientifically useful (see the figure). Indeed, even most statistically "successful" calculations of power laws offer little more than anecdotal value.

By power-law behavior, one typically means that some physical quantity or probability distribution $y(x)$ satisfies (*2*, *3*)

$$y(x) \propto x^{-\lambda} \text{ for } x > x_0,$$

where λ is called the "exponent" of the power law. In the equation, the power-law behavior occurs in the tail of the distribution (i.e., for $x > x_0$). A power-law distribution has a so-called "heavy tail," so extreme events are far more likely than they would be in, for example, a Gaussian distribution. Examples of such relationships have been reported in a wide range of situations, including the Gutenberg-Richter law in seismology (*4*), allometric scaling in animals (*5*), the distribution of hyperlinks on the World Wide Web (*6*), the sometimes vehemently refuted (*7*) "scale-free" nature of the Internet (*8*), a purported unified theory of urban living (*9*), patterns of insurgent and terrorist activity (*10*), and (ironically) the paper publication rates of statistical physicists (*11*). A subtlety to note is that this list includes two different types of reported power laws: bivariate power laws like allometric scaling and power-law probability distributions like the paper publication rates.

Power laws in statistical physics emerge naturally from microscopic theories and can be related to observable macroscopic phenomena. A good example is magnetization (*3*). The derivation of a power law suggests that—in a certain ("critical") regime—phenomena do not possess a preferred scale in space, time, or something else: They are, in a sense, "scale free." However, as Philip Anderson pointed out in 1972 (*12*), one must be cautious when claiming power-law behavior in finite systems, and it is not clear whether power laws are relevant or useful in so-called "complex systems" (*13*, *14*). It is important to take a nuanced approach and consider not only whether or not one has or can derive a detailed mechanistic model of a system's driving dynamics, but also the extent of statistical support for a reported power law. One additionally needs to consider empirical support, as theories for power-law behavior arise from infinite systems, and real systems are finite.

The power law reported for allometric scaling stands out as genuinely good (see the figure) (*5*): Not only is there a sound theory underlying why there should be a power-law

[1]Centre for Integrative Systems Biology and Bioinformatics, Imperial College London, London SW7 2AZ, UK. [2]Oxford Centre for Industrial and Applied Mathematics, Mathematical Institute and CABDyN Complexity Centre, University of Oxford, Oxford OX1 3LB, UK. E-mail: m.stumpf@imperial.ac.uk; porterm@maths.ox.ac.uk

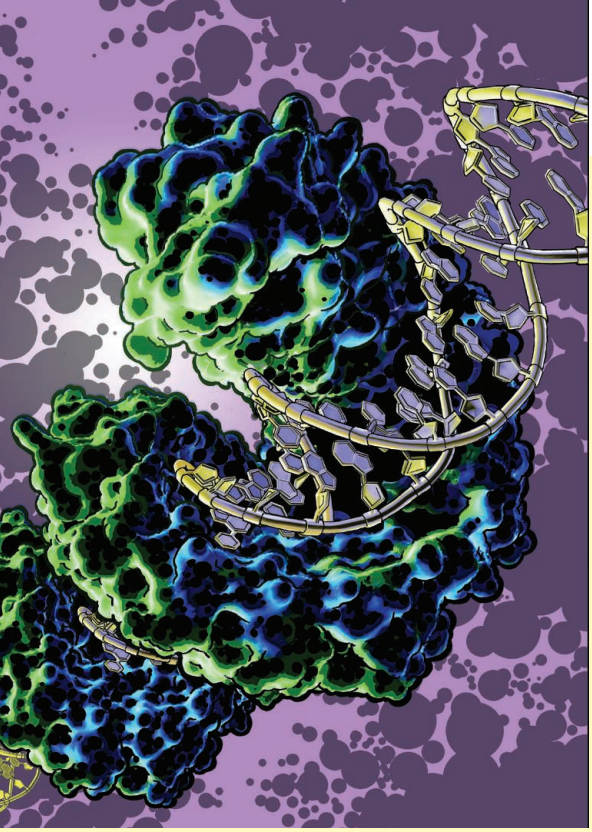

<< Wrapped DNA

TAL effectors are proteins that bacterial pathogens inject into plant cells that bind to host DNA to activate expression of plant genes. The DNA-binding domain of TAL proteins is composed of tandem repeats within which a repeat-variable diresidue sequence confers nucleotide specificity. **Deng *et al.*** (p. 720, published online 5 January) report the structure of the TAL effector dHax3, containing 11.5 repeats, in DNA-free and DNA-bound states, and **Mak *et al.*** (p. 716, published online 5 January) report the structure of the PthXo1 TAL effector, containing 22 repeats, bound to its DNA target. Together, the structures reveal the conformational changes involved in DNA binding and provide the structural basis of DNA recognition.

Spring Bloom

The spring bloom of plankton in northern seas develops apparently in response to increasing light and to winter weather, which make nutrients available at the surface. This seasonality is important on a global scale because it reflects a tipping point, driven by phytoplankton growth, between CO_2 production and carbon storage. The phenomenon is thus of particular interest in this era of carbon excess. **Giovannoni and Vergin** (p. 671) review what is known about the dynamics of these highly ordered microbial plankton communities, discuss the specialist roles of certain taxa, and reflect on predictions for anthropogenic changes to the oceans and what these might mean for geochemical cycles driven by ocean microbiota.

Earthquakes from Above

Preparing for risks and hazards associated with large earthquakes requires detailed understanding of their mechanical properties. In addition to pinpointing the location and magnitude of earthquakes, postmortem analyses of the extent of rupture and amount of deformation are key quantities, but are not simply available from seismological data alone. Using a type of optical remote sensing, Light Detection and Ranging (LiDAR), **Oskin *et al.*** (p. 702) surveyed the surrounding area that ruptured during the 2010 M_w 7.2 El Mayor–Cucapah earthquake in Northern Mexico. Because this area had also been analyzed in 2006, a comparative analysis revealed slip rate and strain release on the shallow fault zone and a number of previously unknown faults. As remote imaging becomes cheaper and more common, differential analyses will continue to provide fault-related deformation data that complements modern seismological networks.

CREDITS (TOP TO BOTTOM): JON BOGDANOVE; KARUNADASA *ET AL.*

Edging In on MoS_2

Molybdenum disulfide is a widely used catalyst in the petrochemical industry that has recently shown promise for water-splitting applications. Its activity appears to be confined to edge sites with exposed disulfide groups, although the precise geometric details underlying the chemistry remain uncertain. **Karunadasa *et al.*** (p. 698) prepared a molecular complex modeling one of these edge sites, in which a triangular Mo-S-S unit is supported by metal coordination to five tethered pyridine rings. The molecule was characterized crystallographically and proved robustly active toward electrochemical generation of hydrogen from water, even when applied to crudely filtered seawater.

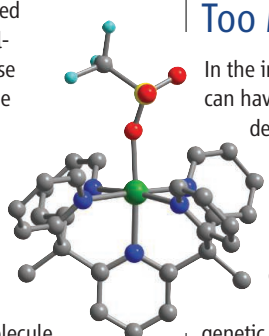

Challenging the Mushroom Bodies

Early memory is labile and is gradually consolidated over time into long-lasting, stable memory. In several species, including mammals, memory consolidation depends on protein synthesis. In *Drosophila*, long-term memory is produced by spaced repetitive training, which induces cyclic adenosine monophosphate (cAMP)–response element–binding protein (CREB)–dependent gene transcription and de novo protein synthesis. Using a large number of genetic tools, **Chen *et al.*** (p. 678; see the Perspective by **Dubnau**) localized this CREB-dependent induction of de novo protein synthesis to two dorsal-anterior-lateral neurons in the adult brain. Importantly, protein synthesis was not required within the mushroom bodies, which are usually considered to be the site of associative learning and memory in insects.

Maintaining Equilibrium

Na^+/Ca^{2+} exchangers (NCX) are membrane transporters that maintain the homeostasis of cytosolic Ca^{2+} and play an essential role in Ca^{2+} signaling. Despite a long history of physiological work and a large body of functional data, the structural basis underlying the ion exchange mechanism of NCX is poorly understood. **Liao *et al.*** (p. 686; see the Perspective by **Abramson *et al.***) present a high-resolution crystal structure of an NCX from *Methanococcus jannaschii* and demonstrate that this archaeal NCX catalyzes Na^+/Ca^{2+}-exchange reactions similar to its eukaryotic counterpart. The structure clarifies the mechanism of ion exchange proteins and reveals the basis for the stoichiometry, cooperativity, and bidirectionality of the reaction.

Too Much Tolerance?

In the immune system, loss of tolerance to self can have devastating consequences, such as the development of autoimmune diseases. In some cases, however, we may wish to be able to break tolerance, for example, to activate immune cells to fight tumors. **Schietinger *et al.*** (p. 723, published online 19 January; see the Perspective by **Lee and Jameson**) used a combination of genetic mouse models and adoptive immune cell transfers to better understand the mechanisms regulating tolerance in T lymphocytes. In contrast to the prevailing paradigm, the maintenance of T lymphocyte tolerance did not require the continuous presence of antigen. Tolerance was able to be broken when previously tolerized cells were placed in an environment depleted of immune cells. However, when lymphocyte numbers were restored, cells were once again tolerized, even in the absence of antigen. These data, together with gene expression profiling, suggest that tolerance

Continued on page 634

Continued from page 633

is associated with a specific gene expression program that, although possible to override temporarily, is reimposed by epigenetic mechanisms.

Be My Guests

For a range of applications, including medical diagnostics or drug delivery, it is necessary to encapsulate one or more components into a microcapsule. While there are many methods that can do this, most either produce a range of capsule size or are not easily scalable for making large quantities. **J. Zhang *et al.*** (p. 690) developed a microfluidic-based system for making capsules using host-guest chemistry. Cucurbit[8]uril, which readily forms complexes in water, was used as the host molecule and could accommodate two different guest molecules. Rapid complexation was observed of methyl viologen–modified gold nanoparticles and a naphthol-containing copolymer.

Ties That Bind

Almost by definition, effective catalysts bind their substrates for a very short time—releasing them quickly after helping them react and then moving on to bind new, as yet unreacted, substrates. This property engenders an efficient cycle, but it hinders study of the binding motif. **Garand *et al.*** (p. 694, published online 19 January; see the Perspective by **Zwier**) devised a technique to extract bound complexes from solution and freeze their conformations in cold, gas-phase clusters. Probing these clusters by vibrational spectroscopy in conjunction with theoretical calculations then allowed the sites of hydrogen bonding that hold the complexes together to be pinpointed.

Close-Up of DNA Methylation

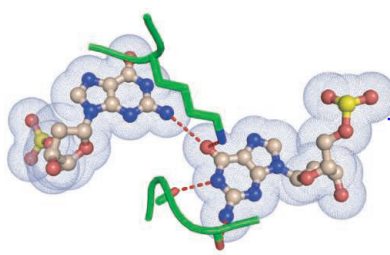

In eukaryotes, maintenance of genomic CpG methylation patterns is required for imprinting, retrotransposon silencing, and X-chromosome inactivation. The epigenetic mark needs to be faithfully maintained and propagated during repeated cell divisions in somatic cells by selective methylation of hemimethylated CpG dinucleotides following DNA replication, which is carried out by the enzyme DNMT1. **Song *et al.*** (p. 709) determined the crystal structure of mouse DNMT1 bound to a DNA duplex containing a hemimethylated CpG on the parental strand, such as would be found immediately after DNA replication. Together with a previous structure of the autoinhibited structure, the findings suggest that a combination of active and autoinhibitory mechanisms ensures the high fidelity of DNMT1-mediated maintenance of DNA methylation.

Before Tohoku-Oki

Recordings by Japan's dense seismic network in the days and weeks before the 2011 M_w 9.0 Tohoku-Oki earthquake provide an opportunity to interrogate what caused the dynamic rupture of one of the largest earthquakes on record. Using a method to extract small earthquakes that are often obscured by overlapping seismic waves, **Kato *et al.*** (p. 705, published online 19 January) identified over a thousand small repeating earthquakes that migrated slowly toward the hypocenter of the main rupture. Based on the properties of these foreshocks, the plate interface experienced two sequences of slow slip, the second of which probably contributed a substantial amount of stress and may have initiated the nucleation of the main shock.

Keeping a Kinase in Check

Cyclic adenosine monophosphate (cAMP)–dependent protein kinase (PKA) is involved in the regulation of several key metabolic pathways. It exists in mammalian cells as an inactive tetramer composed of a regulatory (R) subunit dimer and two catalytic (C) subunits. cAMP binding causes activation by releasing the C subunits. Insight into PKA regulation has come from structures of R and C subunit heterodimers; however, further understanding requires knowledge of the holoenzyme structure. **P. Zhang *et al.*** (p. 712) report a high-resolution structure of the $RII\beta_2$:C_2 tetramer. The structure reveals interactions at an interface between the two RC heterodimers and provides insight into the mechanism of allosteric activation upon cAMP binding.

CREDIT: SONG *ET AL.*